DOKUZ EYLÜL UNIVERSITY
GRADUATE SCHOOL OF NATURAL AND APPLIED SCIENCES

INFLUENCE OF CAPPING LAYER ON THE TRANSFER OF INERTIAL LATERAL LOADS TO JET-GROUT COLUMNS

by
Muharrem KARKILI

November, 2005
İZMİR

INFLUENCE OF CAPPING LAYER ON THE TRANSFER OF INERTIAL LATERAL LOADS TO JET-GROUT COLUMNS

A Thesis Submitted to the
Graduate School of Natural and Applied Sciences of
Dokuz Eylül University
In Partial Fulfillment of the Requirements for
The Degree of Master of Science in Civil Engineering, Geotechnics Program

by
Muharrem KARKILI

November, 2005
İZMİR

M. Sc. THESIS EXAMINATION RESULT FORM

We have read the thesis entitled **INFLUENCE OF CAPPING LAYER ON THE TRANSFER OF INERTIAL LATERAL LOADS TO JET-GROUT COLUMNS** completed by **Muharrem KARKILI** under supervision of **ASSISTANT PROFESSOR DR. GÜRKAN ÖZDEN** and we certify that in our opinion it is fully adequate, in scope and in quality, as a thesis for the degree of Master of Science.

Yard. Doç. Dr. Gürkan ÖZDEN

Supervisor

Prof. Dr. Arif Ş. KAYALAR

(Jury Member)

Prof. Dr. Zafer AKÇIĞ

(Jury Member)

Prof.Dr. Cahit HELVACI
Director
Graduate School of Natural and Applied Sciences

ACKNOWLEDGMENTS

The author would like to express his grateful to the advisor of this thesis, Assistant Professor Dr. Gürkan ÖZDEN, for his invaluable contributions, great supports, helps and advises during his graduate study.

Also, the author would like to thank to Research Assistant Dr. Mehmet KURUOĞLU for his help.

Finally, the author acknowledges gratefully his parents Ahmet and Havva KARKILI and his wife Fatma Nur for their endless support, understanding and patience to his all matters since the beginning.

The author hopes that this study of behavior of capping layer under seismic loads in this dissertation will be useful for next studies.

Muharrem KARKILI

INFLUENCE OF CAPPING LAYER ON THE TRANSFER OF INERTIAL LATERAL LOADS TO JET-GROUT COLUMNS

ABSTRACT

Soil improvement methods using jet-grouting method have been extensively used over the last decade. As in other soil improvement methods, the main reason in the soil improvement with jet grout is to improve the soil parameters in the field. Though the performance of jet grout columns against liquefaction and settlement problems has been found efficient in the 1999 Marmara Earthquake, analysis procedures regarding this method still needs further studies. There are reasons to justify this opinion:

- First of all jet-grout columns are produced by mixing an injection material (a cement-water mixture) with the in situ soil under high pressure.
- Due to its manufacturing method it does not involve major reinforcement and there are variations in sectional parameters along the column length.

Although it is a soil improvement method, jet-grout pile disposition, length and diameter are mostly decided for using pile foundation design principles. In fact the columns are expected to improve the field soil parameters in an average sense. However, end-users tend to treat jet-grout columns as if they are load-bearing elements, question their ability to resist seismic loads. This tendency is understandable since columns are produced in vertical position resembling pile foundations and failure of multiple columns in a treated area may result in differentiable settlement of the structure. The engineer needs to identify the loads acting on jet grout columns and consequent sectional forces in order to design jet-grout columns more realistically. In this thesis influence of the capping layer on the transfer of inertial loads to jet-grout columns has been investigated. It is found that magnitude of lateral load at the column heads is significantly reduced and much less than the assumed values in current design practice.

Keywords: Soil improvement method, jet grout column, inertial lateral load, capping layer.

JET-GROUT KOLONLARA AKTARILAN YANAL ATALET YÜKLERİNDE BAŞLIK DOLGUSUNUN ETKİSİ

ÖZ

Jet grout metodu kullanılarak yapılan zemin iyileştirme yöntemleri, 10 yılı aşkın bir süredir oldukça yaygın olarak kullanılmaktadır. Diğer zemin iyileştirme yöntemlerinde olduğu gibi, jet groutla zemin iyileştirmelerdeki ana neden sahadaki zemin parametrelerini iyileştirmektir. 1999 Marmara Depremi'nde jet-grout kolonlarının sıvılaşma ve oturma problemlerine karşı etkili olduğunun bulunmasına rağmen (Özsoy, 2002), bu yöntemle ilgili hala, yapılacak işler vardır. Bu düşünceyi haklı çıkaran nedenler ise aşağıdaki şekilde sıralanabilir:

- İlk olarak jet-grout kolonlarının, yüksek basınç altındaki malzemenin (su-çimento karışımı) sahadaki zeminin içine bir karışım enjeksiyonu yoluyla üretilmesidir.

- Kolonların üretim metodundan dolayı, eğilme donatısı kullanılamaz ve kolon uzunluğu boyunca kesit parametreleri değişkendir.

Bir zemin iyileştirme metodu olmasına rağmen; jet-grout kolon yerleşimine, uzunluğuna ve çapına, çoğunlukla kazıklı temel tasarım prensipleri kullanılarak karar verilir. Gerçekte, kolonların sahanın zemin parametrelerini ortalama anlamda iyileştirir. Buna rağmen, son kullanıcılar jet-grout kolonlar yük taşıyan elemanlarmış gibi bunların tekrarlı yüklere karşı koyabilme kabiliyetini sorgularlar. Kolonların dikey pozisyonda üretilmesi ve bir bölgedeki bir çok kolondaki olası göçmenin yapının farklı oturmasına yol açma riskinden dolayı bu davranış anlaşılabilir.

Mühendisin jet grout kolonları daha gerçekçi tasarlaması için bunlara etkiyen yüklere ve bunlara bağlı olarak oluşan kesit kuvvetlerini belirlemeye ihtiyacı vardır. Bu tezde, jet-grout kolonlara, atalet yüklerinin aktarılmasında başlık dolgusunun

etkisi araştırıldı. Kolon başındaki yanal yük büyüklüğünün önemli derecede azaldığı ve mevcut tasarım uygulamasındaki kabul edilen değerlerden çok daha düşük olduğu bulundu.

Anahtar Kelimeler: zemin iyileştirme yöntemi, jet-grout kolon, yanal atalet yükleri, başlık dolgusu

CONTENTS

Page

CHAPTER ONE

INTRODUCTION

Soil improvement methods using jet-grouting method have been extensively used over the last decade. Although, it has enjoyed widespread national attention as a fast and economic soil improvement method following the 1999 Marmara Earthquake, there are certain aspects that need to be classified for the design of jet-grout columns.

Customers still have not developed a full confidence for the method since they are skeptical about lateral load carrying capacity of the jet-grout (JG) columns during earthquakes. This debate mainly originates from the fact that JG columns do not involve load-carrying reinforcement. On the other hand, there are case histories demonstrating good performance of JG columns during earthquakes. Field investigations have shown that Soil Crete columns have kept their vertical positions following the Marmara Earthquake. Some cracks along the column lengths were related to dynamic loadings but there were no major failures. The controversy needs to be solved. Therefore, the subject deserves investigation in order to establish well-defined design procedures and to increase customer confidence to the jet-grouting method.

A previous study has shown that JG columns may carry kinematical bending moments if they have enough flexural strength. Testing several bending test samples of JG columns and comparing laboratory strength values with those of the analyses and field findings may clarify this aspect of JG behavior under seismic loads.

The inertial lateral loads, however, appears to be exceeding lateral load carrying capacity of JG columns according to currently applied analysis methods. It is assumed that bending moments do not take place at the column heads and the shear force at the bottom of the raft foundation fully acts at the column level in direct proportion to column spacing. This assumption seems to be over conservative considering the damping potential of the capping layer and positive behavior of the

columns in previous earthquakes. Because of these reasons this thesis study targets the transfer of inertial loads to the JG columns. Namely the influence of the capping layer was studied in numerical analyses stage of the thesis.

In the second chapter of the thesis a case history regarding earthquake performance of JG columns is given. It is demonstrated that columns in the Ford Plant site in Gölcük did not completely fail in the 1999 Marmara Earthquake. (Özsoy, 2002) The third chapter is devoted to the statement of the problem and modeling aspects. Results are presented and discussed in the fourth chapter. The thesis ends with the final conclusion chapter. Details of the finite element analyses are given in the appendix.

CHAPTER TWO

CASE STUDIES

2.1 Introduction

Case studies are essential in understanding performance of jet grout columns in the field during earthquakes. In the following sections case history (Özsoy, 2002) of an industrial plant during the 1999 Marmara Earthquake is given.

2.2 Ford-Otosan Gölcük Plant

2.2.1 Site Description

The Ford Otosan Gölcük Plant is located in the southern coast of the gulf of İzmit, in Gölcük district, which is one of Turkey's industrial regions.

The site is formed by alluvial soils, which are transported by the river passing along the border of the site. The field in the plant is sloped from south toward north.

In addition to administrative and ancillary buildings, there are five major structures located on the site - Press, Body, Paint, Assembly Shop and Supplier Park buildings.

After the 17th of August 1999 Marmara Earthquake with a magnitude M=7.4, the surface faulting occurred along the southern border of the plant area causing differential tectonic settlements in addition to 1.6 m of overall vertical drop of the plant site. It should be noted that the plant was also subject to 1999 Düzce Earthquake. General characteristics of these earthquakes are given in Table 2.1. The buildings made before the earthquake and the location of the fault line are given in Figure 2.1.

Table 2.1 Characteristics of 1999 Marmara and Düzce Earthquakes

Features	Kocaeli	Düzce
Date of Event	17/08/1999	12/11/1999
Magnitude	$M_w = 7.4$	$M_w = 7.1$
Type	right lateral strike slip	right lateral strike slip
Surface Rupture (m)	Max.: 5.5 / Avg.: 3.5	Max.: 5.0 / Avg.: 3.0
Length (km)	126	40
Peak Ground Acceleration (PGA)	0.45g	0.80g
Duration (s)	45	20

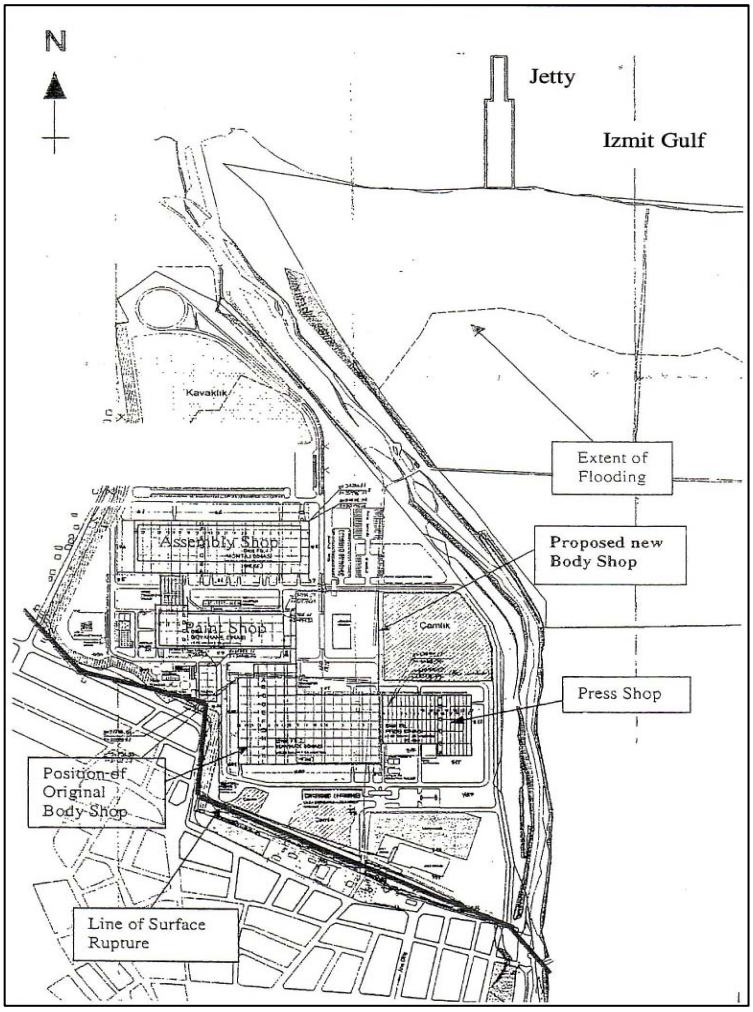

Figure 2.1 Site plan and the location of the fault line. (Özsoy, 2002)

2.2.2 Soil Conditions

The soil profile in the field consists of alluvial deposits of İzmit-Sapanca alluvial basin of which average thickness is said to be 200 m. The field has been a forest prior to the construction campaign. Further soil borings following the Marmara Earthquake showed silt, clay, sand and gravel soil layers in the field. It is also interesting to note that natural gas has been encountered during hydro geological explorations. It was noted in the original report that the gas was either a product of organic soil deposits or came from the fault line. It is understood that the faulting regime in the history might have controlled the sedimentation in the area. Sudden submergence of the land into the sea caused deposition of marine soils followed by river originated alluvial soils.

2.2.2.1 Site Specific Soil Investigations

A geotechnical investigation was performed in the plant site in 1998 prior to the construction activities. Borehole locations can be seen in Figure 2.2. It was mentioned in the aforementioned reference that soil idealization was based on the following boreholes (Table 2.2). The Standard Penetration Test (SPT) blow count variations with depth for the Old Body and Paint shops are given in Figure 2.3 and Figure 2.4, respectively. As one can notice in the figures relative density of the soil layers in the profile vary in a wide range. Consistency limit tests of cohesive soil samples showed that such soils fall in the low plasticity clay (CL) group. It was found based on the findings of grain size distribution analyses of the coarse grained samples that such samples contain considerable amount of fine content, which is no less than 20% for the majority. Details of index tests can be seen in the referred text (Özsoy, 2002). Based on extensive site investigation studies including cone penetration tests it can be said that the site has been a typical example to alluvial deposits with horizontal layering discontinuities and alternating sand, silt, clay layers.

Table 2.2 Boreholes on which soil idealization was based

Location in the Plant	Boreholes
Body Shop	S3,S4,S5,S6,S7,S8,S9,S10
Paint Shop	*S9,S10,S11,S12*

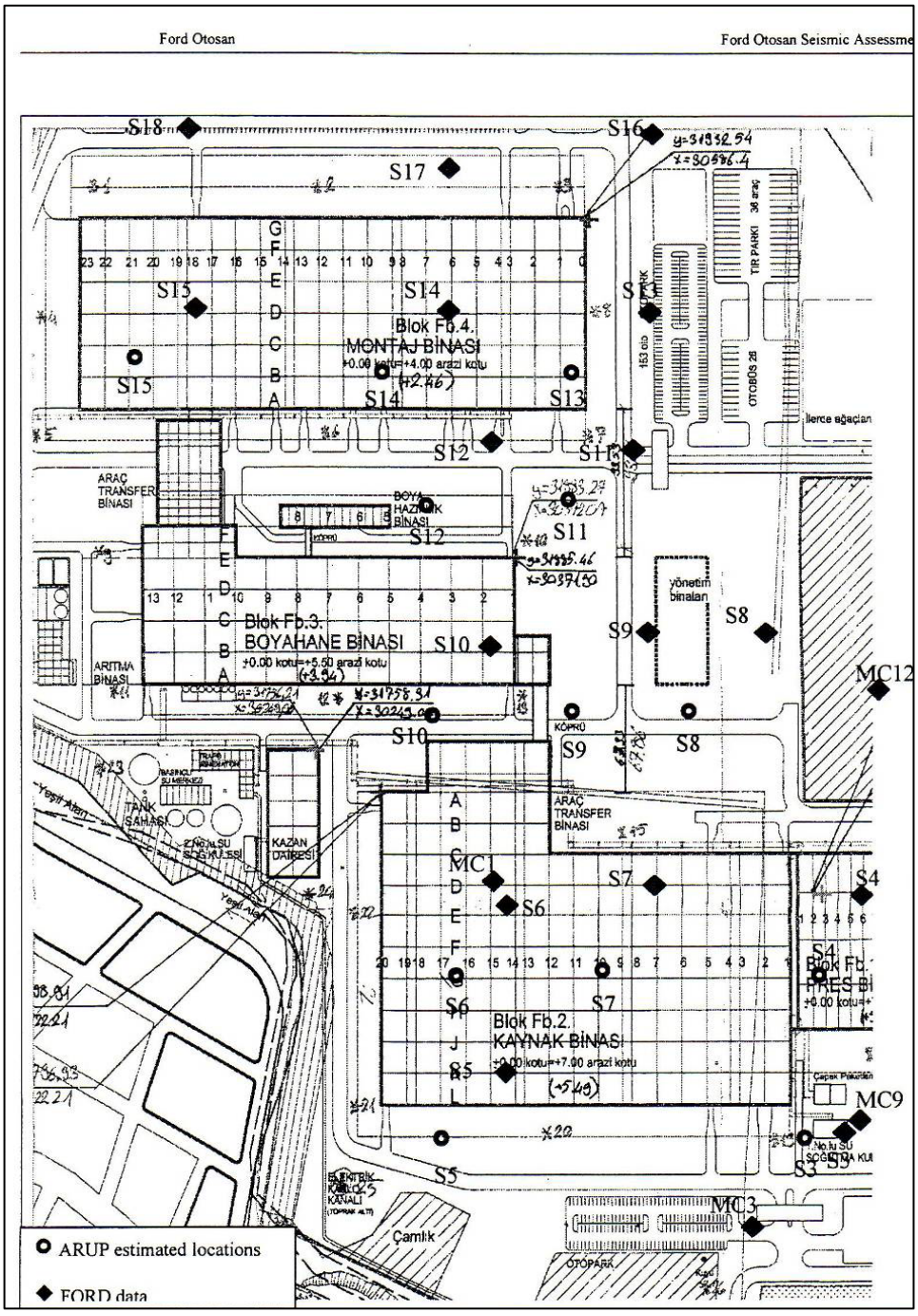

Figure 2.2 Borehole locations that were drilled before the earthquake. (Özsoy, 2002)

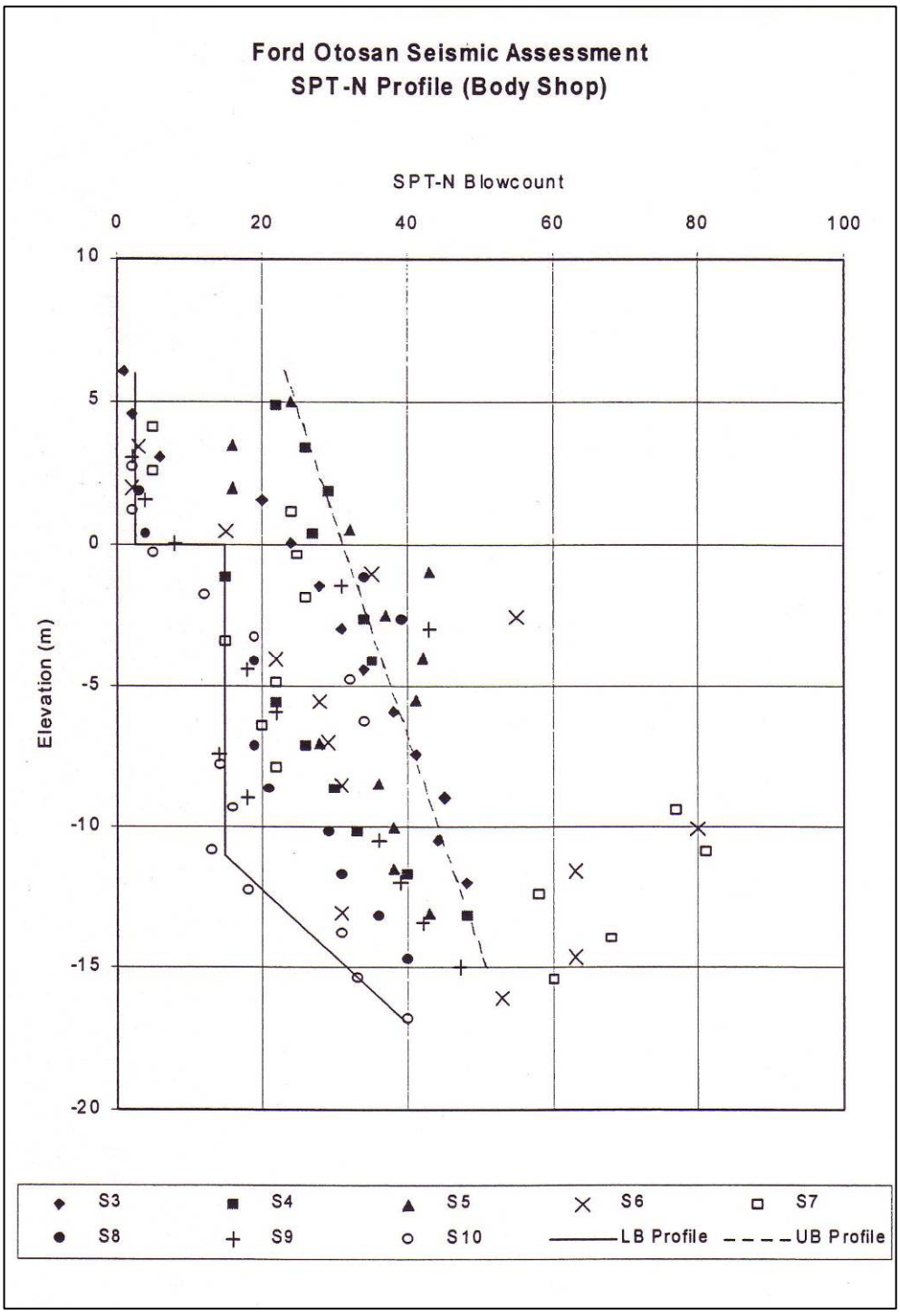

Figure 2.3 Variation of SPT-N values at Old Body Shop location. (Özsoy, 2002)

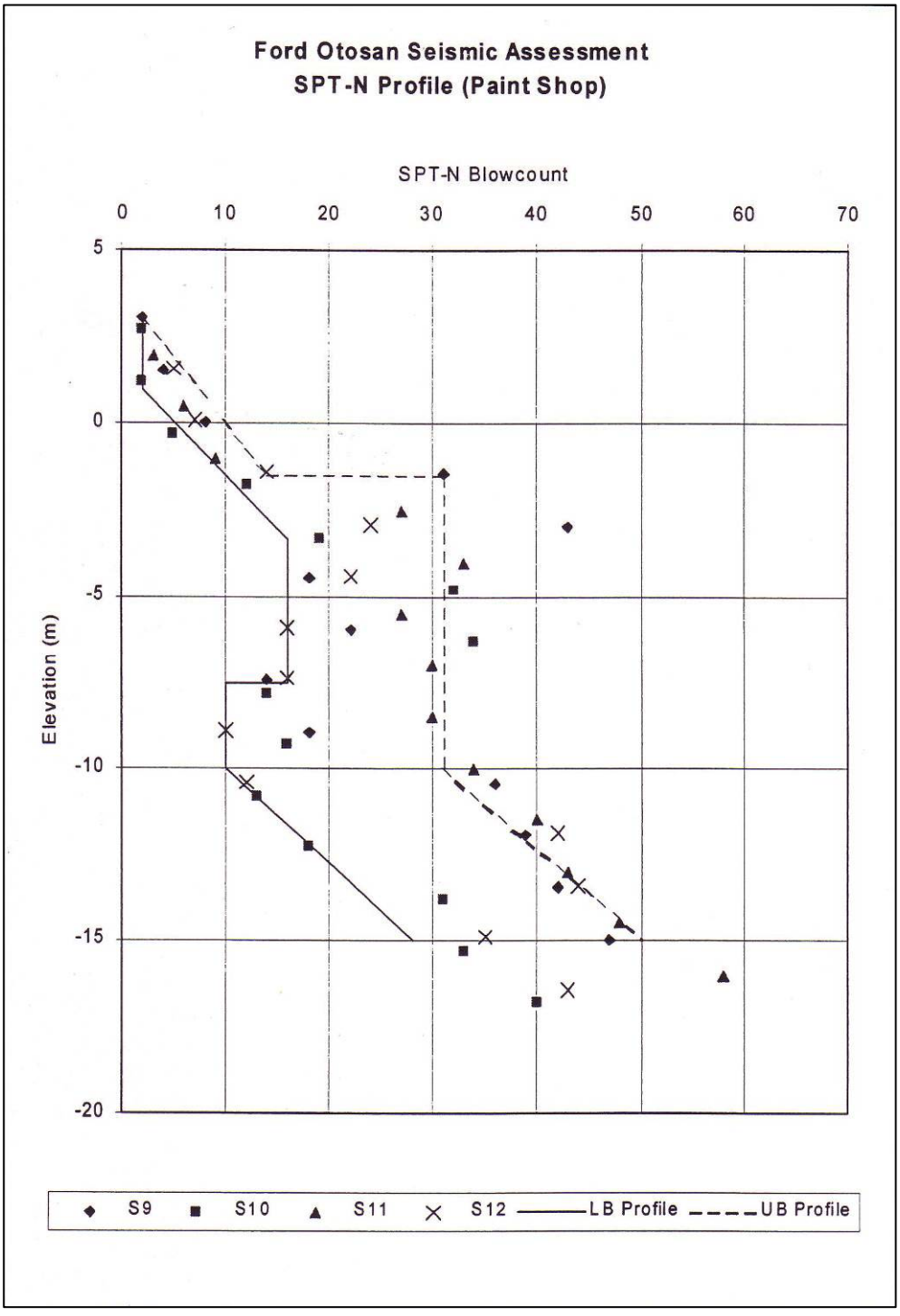

Figure 2.4 SPT-N variations at the Paint Shop location. (Özsoy, 2002)

2.2.3 Geotechnical Design Parameters

Idealized soil profile in the Ford Plant site was given in separate tables for the northern and southern regions. (Özsoy, 2002) It was stated in the mentioned reference that soil boring logs, SPT blow counts and CPT findings were used in the generation of these idealized profiles (Table 2.3 and Table 2.4).

Table 2.3 Southern Idealized Soil Profile 1

Layer Number	Layer Thickness (m)	Description
1	3.0	Soft sandy silty CLAY
2	4.0	Medium dense silty SAND
3	3.5	Medium stiff clayey SAND
4	4.7	Dense silty SAND with gravel
5	1.4	Stiff clayey SILT
6	4.4	Dense silty SAND with gravel
7	-	Dense silty SAND

Table 2.4 Northern Idealized Soil Profile 2

Layer Number	Layer thickness (m)	Description
1	3.5	Very soft silty CLAY
2	5.5	Firm clayey SILT
3	3.5	Soft to stiff clayey SILT
4	2.0	Firm silty CLAY
5	6.5	Stiff clayey SILT
6	-	Stiff clayey SILT

It is seen in the above given tables that the southern area of the plant consists of sandy soils whereas the northern area involves dominantly cohesive soil layers.

Static and dynamic soil parameters were based on in situ and laboratory tests. Results are tabulated and plotted as in the following:

Table 2.5 Static Soil Parameters (Soil Profile 1). (Özsoy, 2002)

Layer Number	**Elevation (mRL)**	***SPT-N*** **(N_{60})**	**Friction Angle**	**S_u (kPa)**	**Unit Weight (kN/m^3)**	**PI (%)**
1	4.0 to 1.0	9	28°	45	18	20
2	1.0 to -3.0	25	35°	-	19	-
3	-3 .0 to -6.5	20	31 °	-	19	I 5-20
4	-6.5 to -11.2	29	35°	-	19	-
5	-11.2 to -12.6	23	31 °	100	19	15-20
6	-12.6 to -17.0	40	38°	-	19	-
7	Below -17.0	40	38°	-	19	-

Table 2.6 Static Soil Parameters (Soil Profile 2). (Özsoy, 2002)

Layer Number	**Elevation (mRL)**	**SPT-N (N_{60})**	**Friction Angle**	**S_u (kPa)**	**Unit Weight (kN/m^3)**	**PI (%)**
1	4.0 to 0.5	3	26°	10	18	20-30
2	0.5 to -5.0	17	28°	50	19	15-20
3	-5.0 to -8.5	10	26°	15 + 11.25z	19	15-20
4	-8.5 to -10.5	$q_c \approx 1MPa$	-	50	19	15-20
5	-10.5 to -16.5	-	26°	76 + 11.25z	19	20-25
6	Below-16.5	30 to 50	26°	150	19	20-25

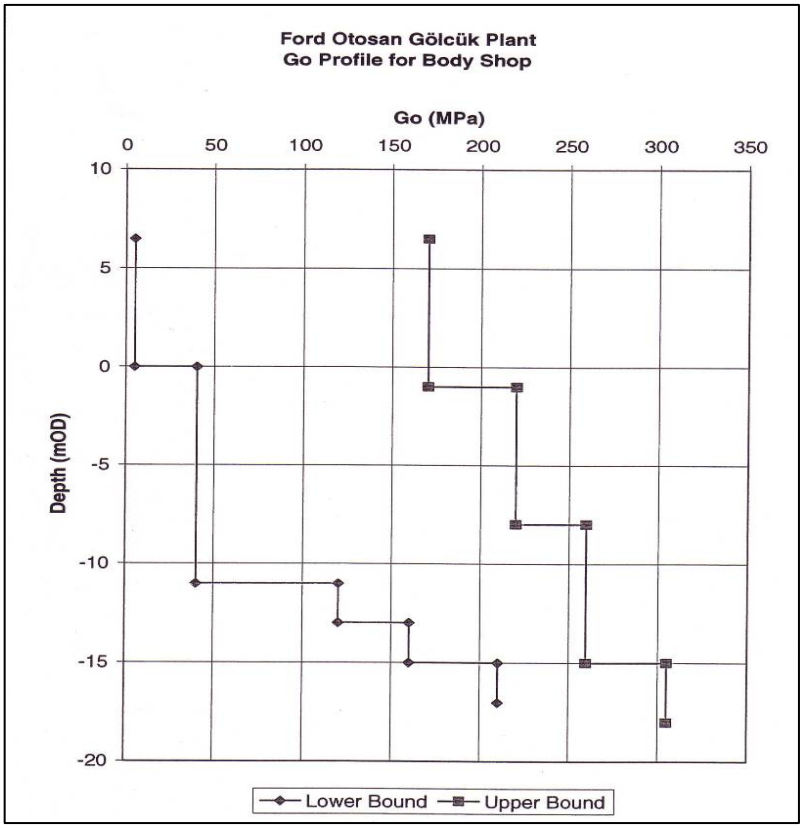

Figure 2.5 Shear modulus, G_o, Profile for the Old Body Shop(özsoy,2000)

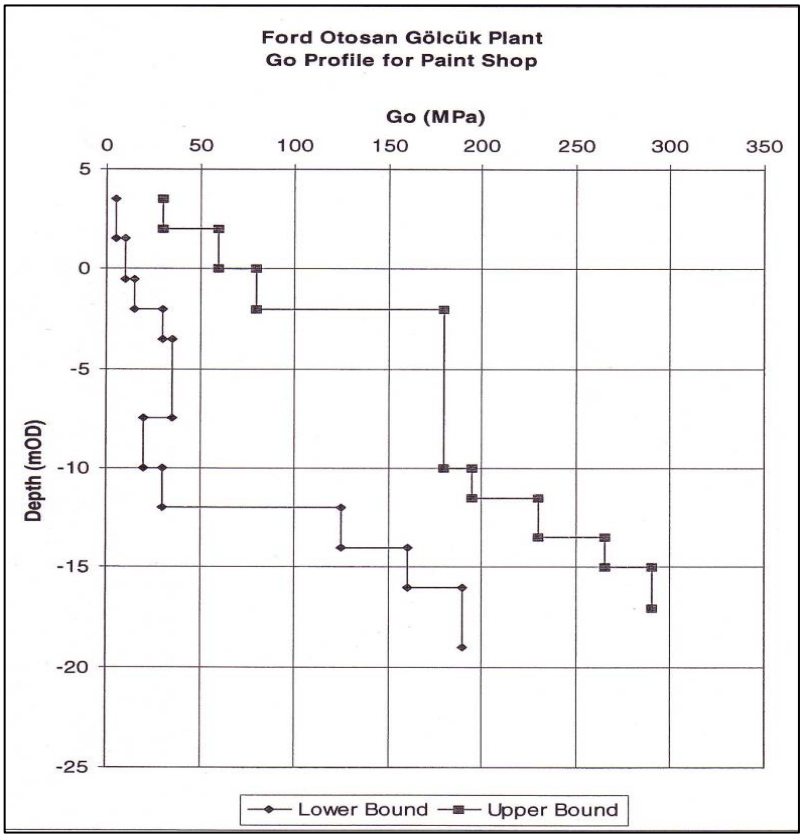

Figure 2.6 Shear modulus, G_o, Profile for the Paint Shop (Özsoy,2000)

Table 2.7 Maximum shear modulus/Undrained shear strength ratio, (G_o/S_U). (Kramer,1996)

PI (%)	Over consolidation ratio, OCR		
	1	2	5
15-20	1100	900	600
20-25	700	600	500
34-45	450	380	300

2.2.4 Liquefaction in the Hazard Site

Following the 1999 Marmara Earthquake liquefaction related deformations were observed in the site. For instance lateral spreading along the shoreline has been reported to take place (Özsoy, 2002). In addition to this some sand boils have been observed between the Paint and Assembly shops. The lateral spreading has caused 3 to 5 meters of permanent deformations towards the sea resulting in the submersion of some portions of the site. Submerged areas of the site were then backfilled.

Figure 2.7 Lateral spreading along the shoreline (Özsoy, 2002)

2.2.5 Performance of soil Improvement Techniques at the Site

Although there are signs for liquefaction and observed differential settlements within the buildings are attributed to local liquefaction problems, it is believed that previously applied soil improvement techniques helped to reduce this effect (Özsoy, 2002). However, it is highly likely that extensive liquefaction did not take place in the site. Probably it only occurred in small pockets.

Liquefaction risk has been foreseen for the site before the earthquake and remedial measures were taken. Selected soil improvement techniques for the site were stone column and jet grouting applications.

The center-to-center spacing for jet grout columns located in the relatively lightly loaded areas (i.e. JG columns loaded up to 20 kPa in the Body Shop) was 2.7 m whereas it was 2.0 m in the heavily loaded zones of the Press Shop (i.e. up to 50 kPa). Pull-out and zone loading tests performed in the site resulted in successful jet grout column performance.

Following the 1999 Marmara Earthquake a damage assessment program was pursued in the site. Core samples were taken from columns. It was seen that most columns kept their vertical positions although some of them were detected as damaged due to earthquake related soil deformations. A zone-loading test was made on four JG columns, which were loaded up to 2600 kN. The test ended with a permanent settlement of 6 mm showing successful performance of the JG columns during the earthquake.

CHAPTER THREE

STATEMENT OF THE PROBLEM

3.1 Introduction

Soil improvement methods using jet-grouting method have been extensively used over the last decade. As in other soil improvement methods, the main reason in the soil improvement with jet grout is to improve the soil parameters in the field.

In jet grouting method problematic soils are improved by mixing in-situ soils with high pressure cement grout through nozzles on rotating pipes that are being withdrawn to the ground surface at a constant speed. In the field, injection equipment is pushed down to the target depth using hydraulic force. While hydraulic pressure is used to push the equipment to the target depth, pressurized water is also utilized to erode the soil. The target depth may be defined as the bottom elevation of jet-grout columns. The method is widely recognized and applied nationally since soil Crete columns at varying dimensions (both in terms of length and diameter) can be produced relatively economically and quickly. Jet-grouting process and its potential application styles are given in Figures 3.1 and 3.2, respectively.

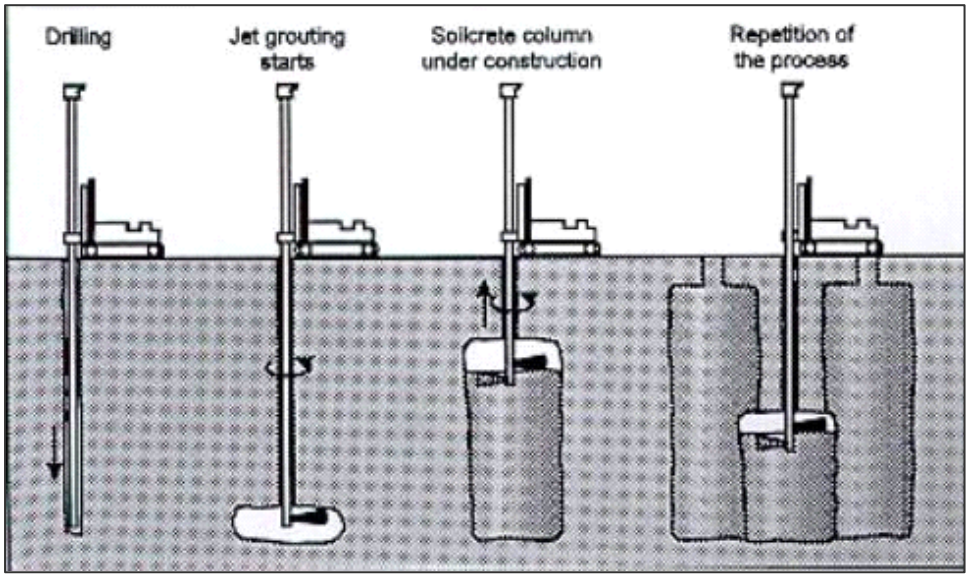

Figure 3.1 Illustration of jet-grouting application (Hayward Baker Company, 2005)

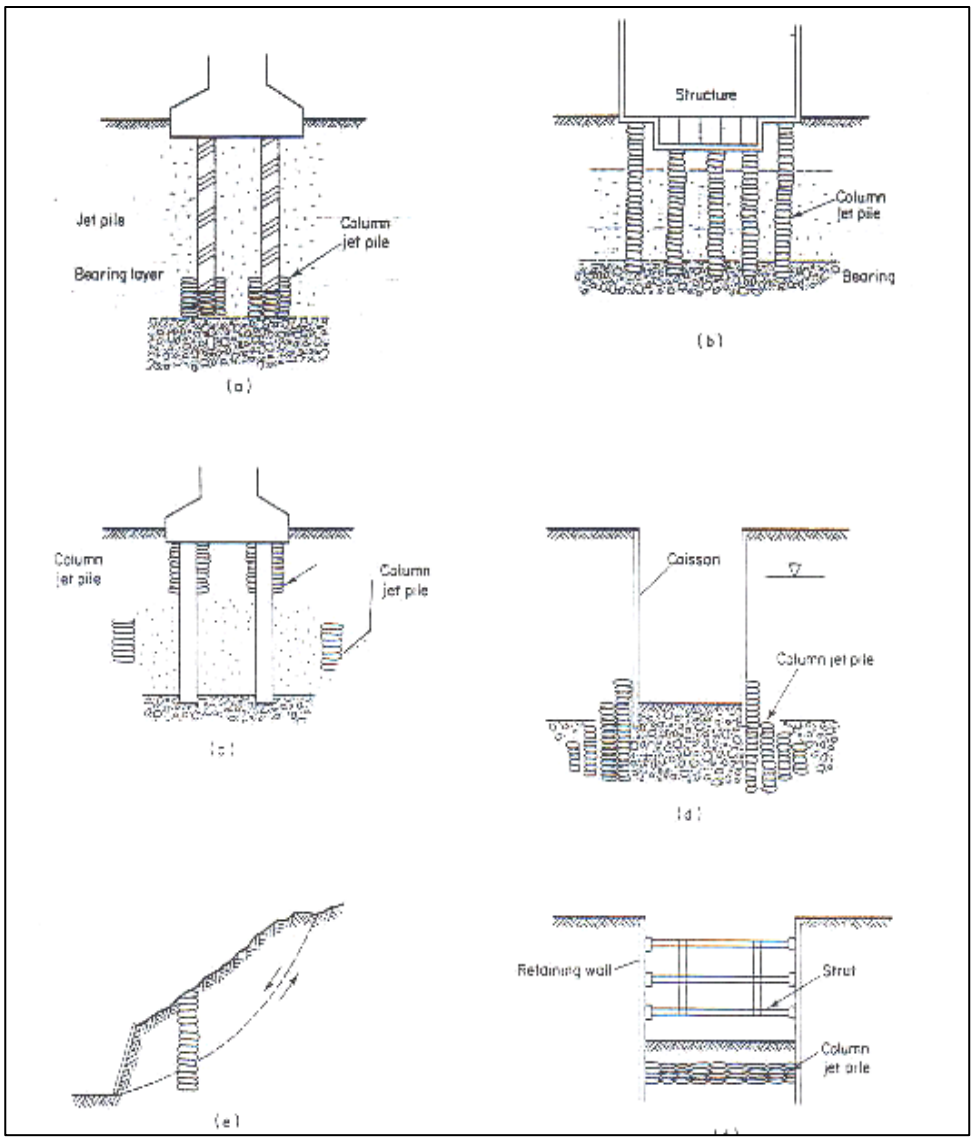

Figure 3.2 Potential application areas of jet-grouting method

3.2 Problems Associated with Jet-Grout Column Design

Though the performance of jet grout piles against liquefaction and settlement problems has been found efficient in the 1999 Marmara Earthquake as explained in the previous chapter, analysis procedures regarding this method still needs further study due to following reasons:

a. Jet-grout columns are produced by mixing an injection material (a cement-water mixture) with the in situ soil under high pressure. Due to its

manufacturing method it does not involve major reinforcement and there are variations in sectional parameters along the column length.

b. Although it is a soil improvement method, jet-grout pile disposition, length and diameter are mostly decided for using pile foundation design principles. In fact the columns are expected to improve the field soil parameters in an average sense. However, end-users tend to treat jet-grout columns as if they are load-bearing elements question their ability to resist seismic loads. This tendency is understandable since columns are produced in vertical position resembling pile foundations and failure of multiple columns in a treated area may result in differentiable settlement of the structure. Loads acting on jet grout columns and consequent sectional forces have not been fully studied yet.

Seismic lateral loads acting on jet grout columns can be examined in two different categories. These categories can be listed as in the following, and are illustrated by Figure 3.3.

1. Inertial loads due to the seismic action of the superstructure, and
2. Kinematical loads due to the vibration of surrounding soil layers.

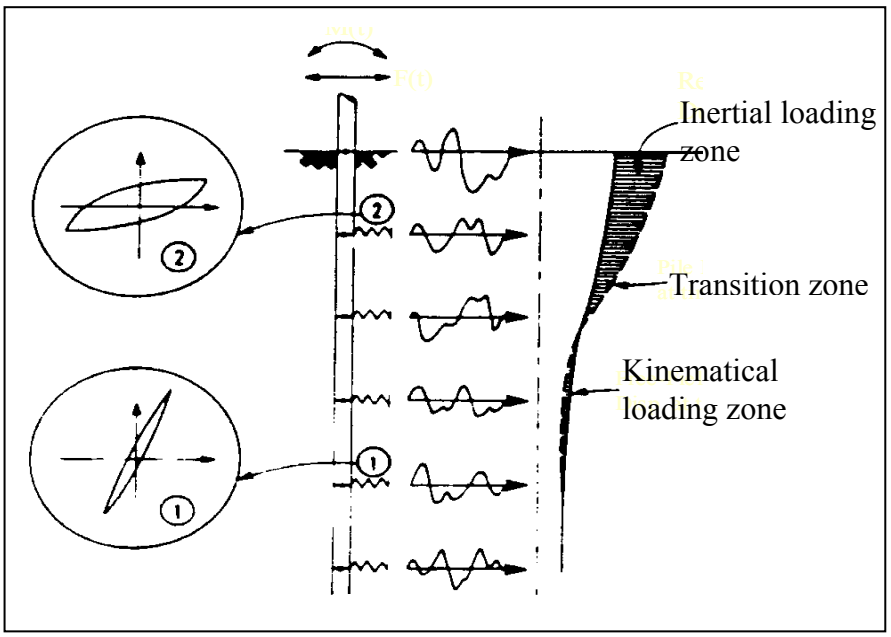

Figure 3.3 Seismic loads acting on jet-grout columns

In conventional pile analysis and design it is assumed that inertial load near the ground surface govern pile behavior unless the soil profile dictates consideration of kinematical loads. A similar philosophy can also be followed for jet-grout column analysis. However, magnitude of the forces can be significantly less than those acting on conventional piles. This is because of two reasons: firstly elasticity modulus of a jet-grout column is several times less than that of a conventional pile; secondly the columns are isolated from the structural foundation by means of a capping layer.

Lower elasticity modulus would provide higher compatibility to the columns with the vibrating soil layers compared with the conventional reinforced concrete piles. This aspect of the jet grout column behavior can be studied using the method by Nikolau and Gazetas (1997). Askay (2002) showed that bending moments on the columns are calculated almost eight times less than RC piles. Analyses parameters and results of Askay are presented in Tables 3.1 and 3.2, respectively.

Table 3.1 Kinematical load analyses parameters of Askay (2002)

h_1 (m)	V_1 (m/s)	V_2 (m/s)	E_{jg} (kN/m^2)	E_{pile} (kN/m^2)	E_1 (kN/m^2)	a_s (m/s^2)	ρ_1 (Mg/m^3)	L (m)	d (m)
11.5	188.9	206.4	1x10^6	2.9x10^7	188,392	2.9	2.9	17	0.6

In the above table ρ_1, E_1, h_1 and V_1 are density, elasticity modulus, thickness and shear wave velocity of the soil layer above the interface at which soil parameters change abruptly resulting in the generation of kinematical bending moments. V_2 is the shear wave velocity of the layer below the interface. E_{jg} and E_{pile} are the elasticity modulus of the jet-grout column and the RC pile. L and d are the pile length and diameter whereas a_s is the maximum ground surface acceleration. It should be noted that assumed elasticity modulus value (1 GPa) for the jet-grout is representative for silty sands and silts. Same parameter was found as 2.7 GPa for the columns in the Ford Plant site. (Özsoy, 2002)

Table 3.2 Kinematical analyses results of Askay (2002)

		kinematical bending moment (kN·m)
jet -grout column	resonant condition	1.63
	non-resonant condition	1.0
reinforced concrete pile	resonant condition	14.5
	non-resonant condition	8.6

The second factor (i.e. separation of the columns from the structural foundation by means of a capping layer) demonstrates its influence on column behavior from the inertial loading point of view. In current design practice columns are designed assuming that shear forces due to the inertial action of the structure are fully transferred to jet-grout column heads in direct proportion to jet grout column spacing. Bending moments at the top of the columns do not occur since structural foundation is free to rotate. The shear forces are converted to equivalent static lateral loading at the top of the column, which was then analyzed according to well known p-y method of the API (1980).

Inertial loads that are actually transferred to the columns are expected to be less than the assumed magnitudes due to the damping effect of the capping layer. Effective period of the inertial vibration frequency, natural period of the structure, thickness of the capping layer and jet-grout column spacing are among the parameters that would influence inertial load transfer to the columns. Among these parameters the capping layer thickness and loading frequency are studied in this thesis study following the below given methodology.

3.3 Analysis Method

In order to study the above given parameters on the inertial loads the preferred method was the finite element method. Plaxis software was used for this purpose. A soil profile considered as typical for soils that need to be improved against dynamic effects. This profile is frequently encountered in the Old Gediz River Delta (Zetas,2001). It is given in Figure 3.4. One should note that only the top 40 m of the profile was investigated. The rest of the profile down to 100 m was assumed as a stiff clay layer with the below given characteristics.

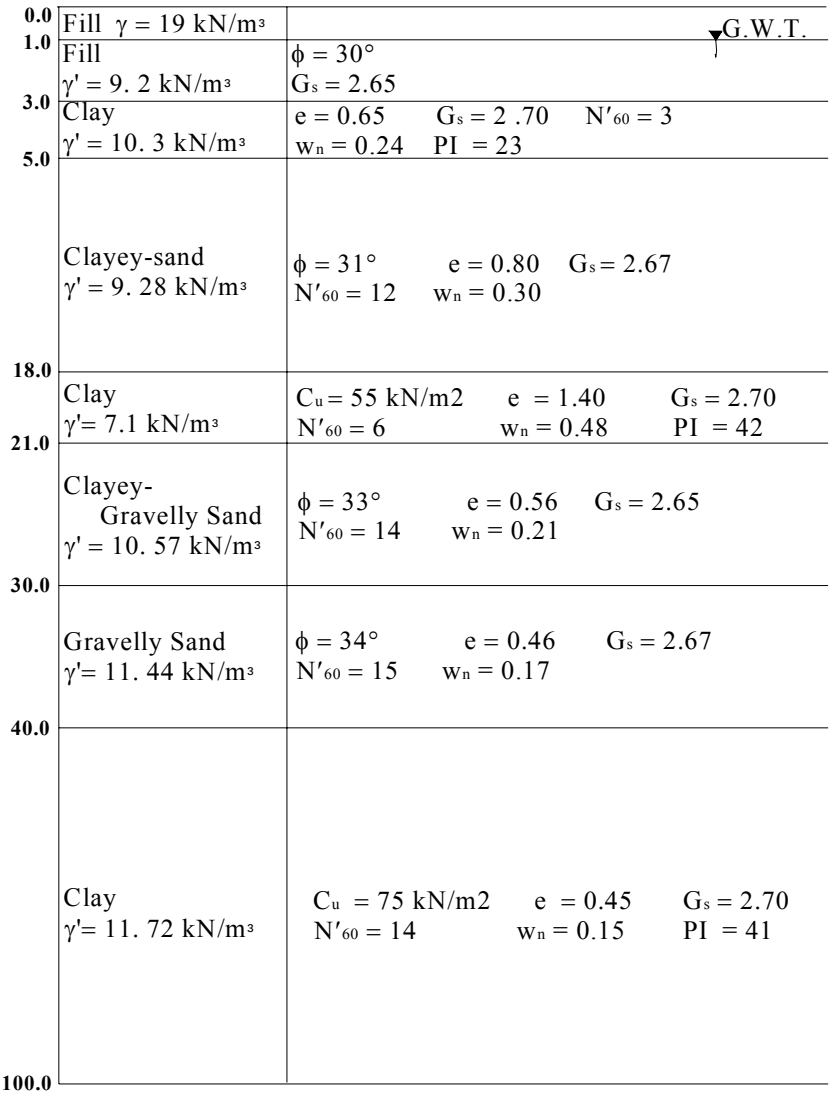

Figure 3.4. Representative soil profile for the study

The soil profile given in Figure 3.4 is further idealized for finite element modeling. The layer thickness to be improved has been chosen as almost 17 m below the capping layer. The structure was a single story building with a rigid girder and a rigid raft foundation. The finite element model was established using plain strain 15 node triangular soil elements. Only the capping layer has utilized nonlinear Mohr-Coulomb soil model so that damping effect of this layer was accounted for. Five columns were placed in the section. Since the column number was kept constant and spacing varied (S=2B, 3B and 4B; B: column diameter), the raft width has become variable. Dynamic loading has been applied as harmonic sine wave with loading periods of 0.1, 0.25, 0.5 and 1.0 seconds. In addition to this equivalent static analysis was also performed where the lateral load was taken as the 20% of the building weight. Transferred shear force to the column top was computed along the interface elements of the FEM model. These aspects of the model are shown in Figure 3.5 and Figure 3.6.

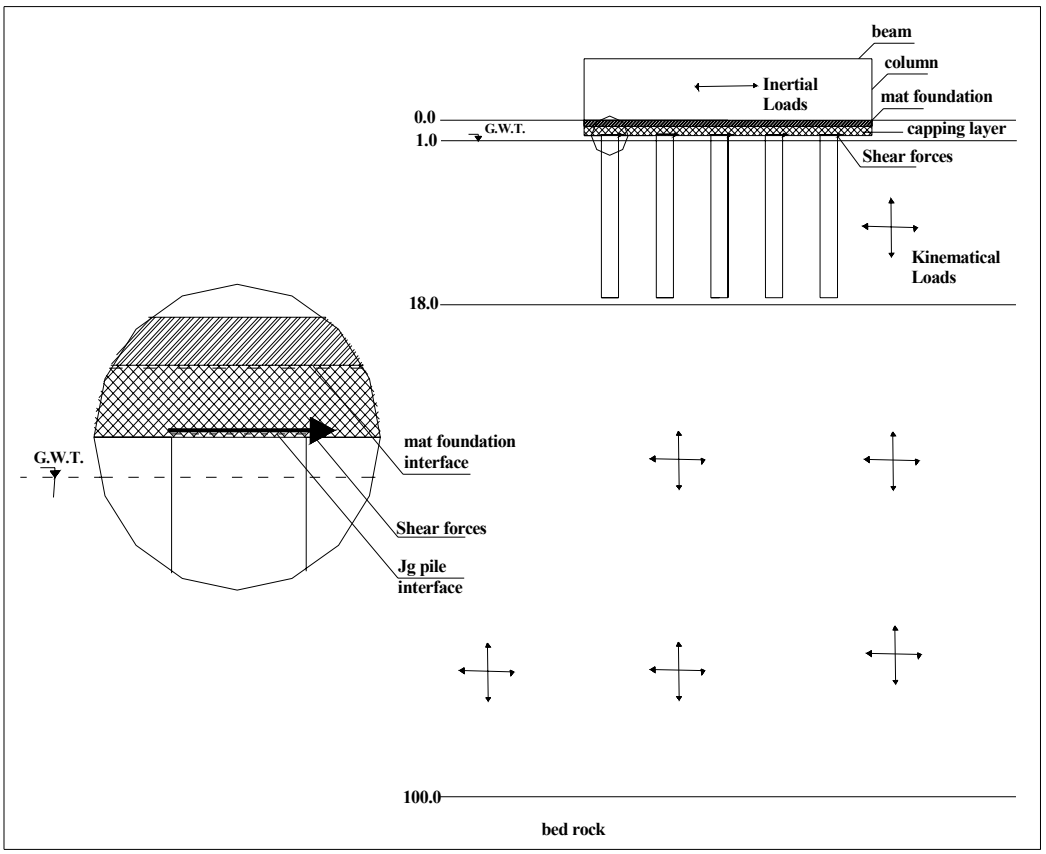

Figure 3.5 Idealized soil profile for the FEM model and capping layer interface details

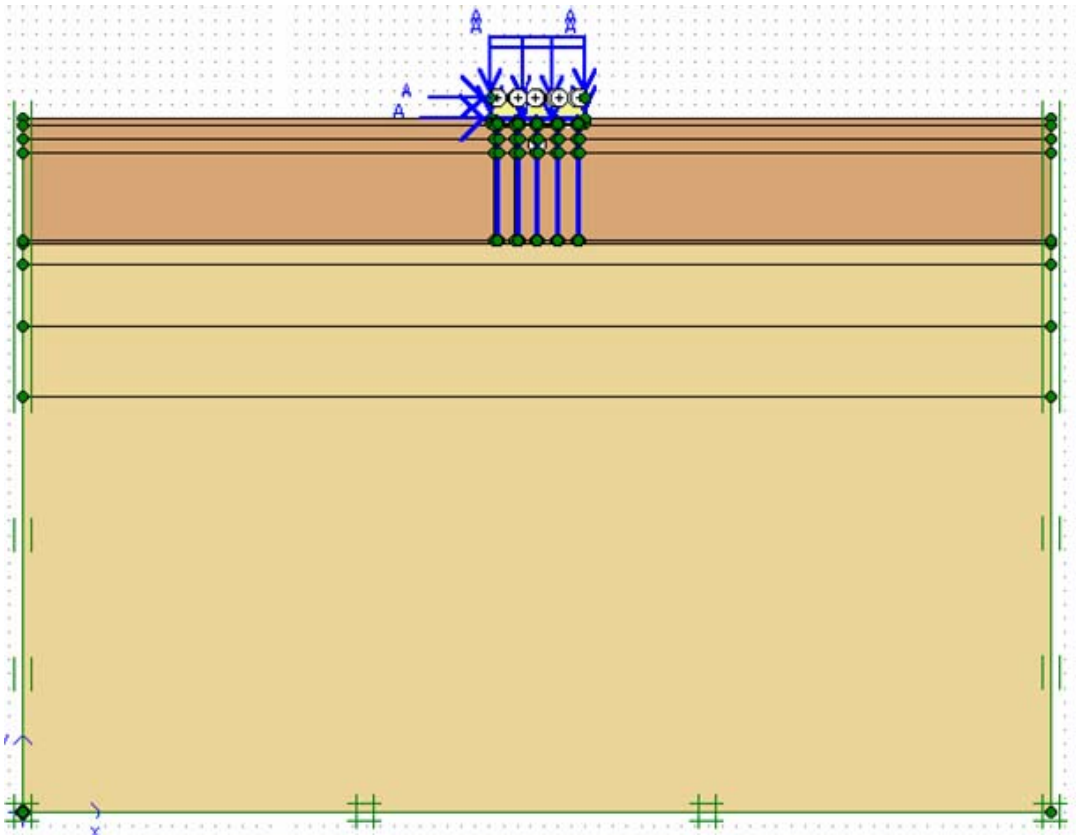

Figure 3.6 Finite element model of the Plaxis software

CHAPTER FOUR

RESULTS AND DISCUSSIONS

In order to study the behavior of jet-grout columns under lateral seismic loads, analyses were carried out using the soil profile with different variations. The variables in the soil profile are:

1. Spacing of jet-grout columns
2. Thickness of capping layer
3. Period of dynamic motion

Analyses were performed using Plaxis 8.0 software, (Brinkgreve, R.B.J, 2002). Figures were prepared in order to evaluate the results of Plaxis analysis. In these figures, combination of shear stresses in interface layers between top of piles and mat foundations, period and jet-grout column spacing variables are shown. These figures were evaluated taking variables into consideration and in connection with constant variables.

Initially, figures in which capping layer thickness is fixed but jet-grout column spacing is variable have been developed (Figures 4.1-4.4). In these figures, the analyses have been carried out for there different periods (T=0.25 s, T=0.50 s, T=1.0 s). Variations were not observed in shear stresses applied on top of columns at T=0.25 s and T=0.50 s periods depending on jet-grout column spacing. However, in the analysis of T=1.0 s period, a sudden increase was observed in level of the shear stress applied on top of the column. The natural period of soil profile (Das, 1993) model was determined as :

$$T = \frac{4 * H}{V_s} \qquad 4.1$$

$$T = \frac{4 * 100}{356} = 1{,}1 \text{ s} \qquad 4.2$$

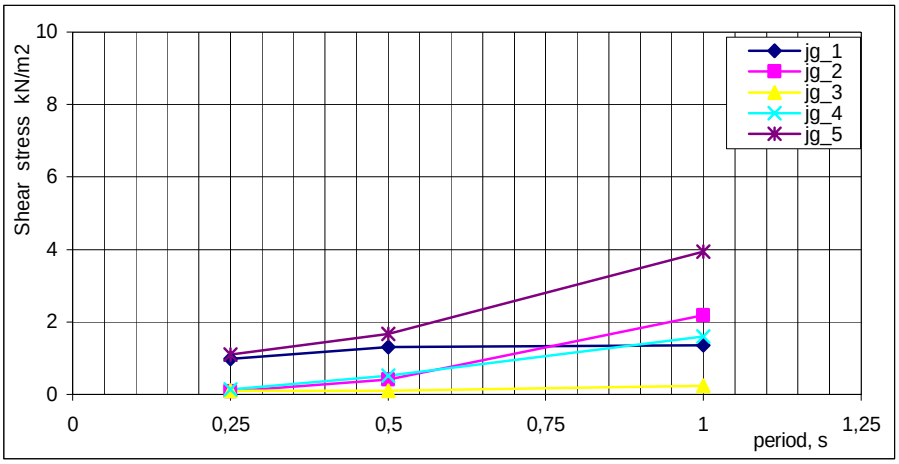

a. capping layer thickness: 10 cm, jg column spacing: 2b

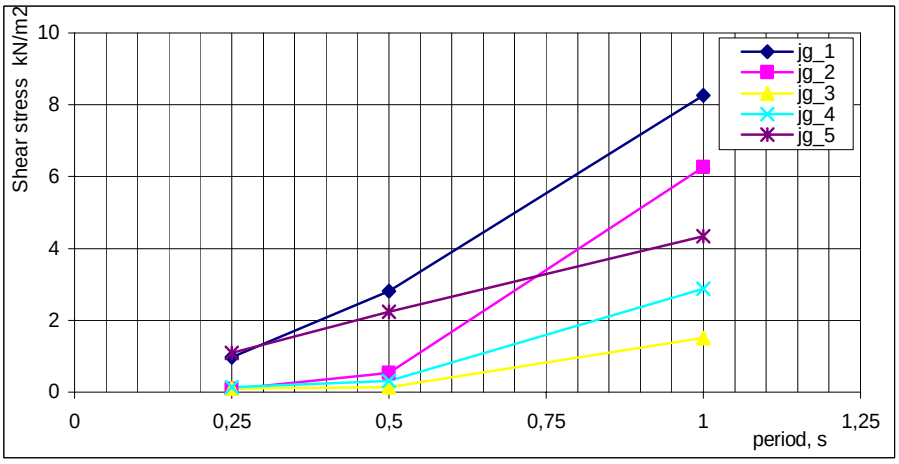

b. capping layer thickness: 10 cm, jg column spacing: 3b

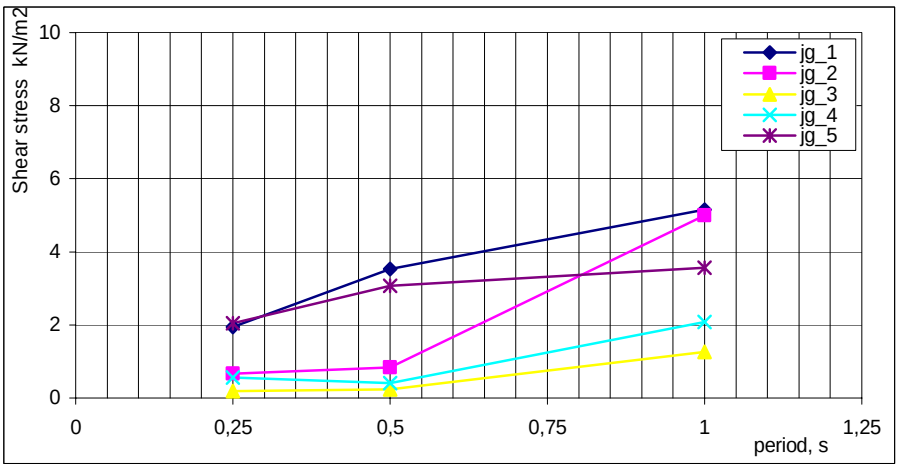

c. capping layer thickness: 10 cm, jg column spacing: 4b

Figure 4.1 Shear stresses applied on top of jg columns depending on jg column spacing, capping layer thickness: 10 cm

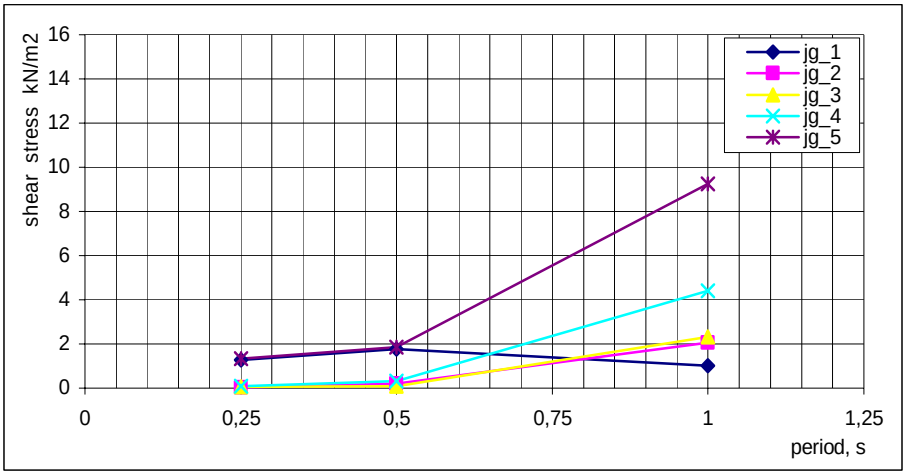

a. capping layer thickness: 30 cm, jg column spacing: 2b

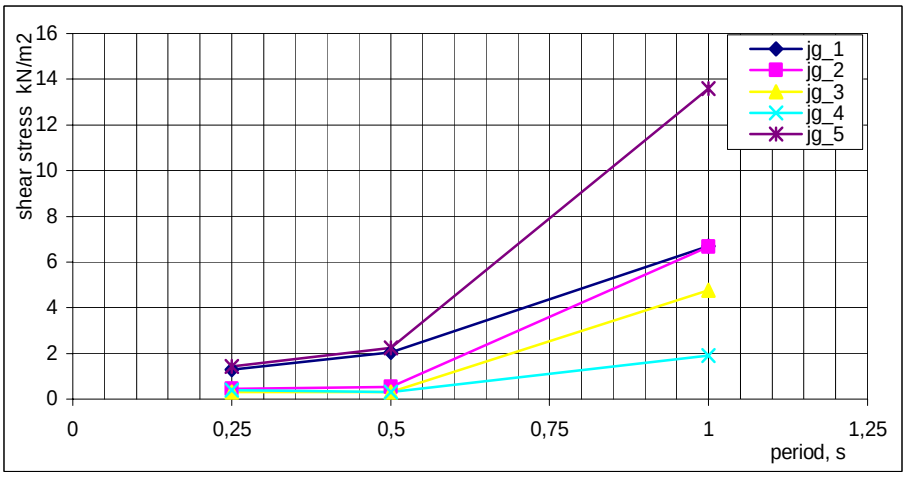

b. capping layer thickness: 30 cm, jg column spacing: 3b

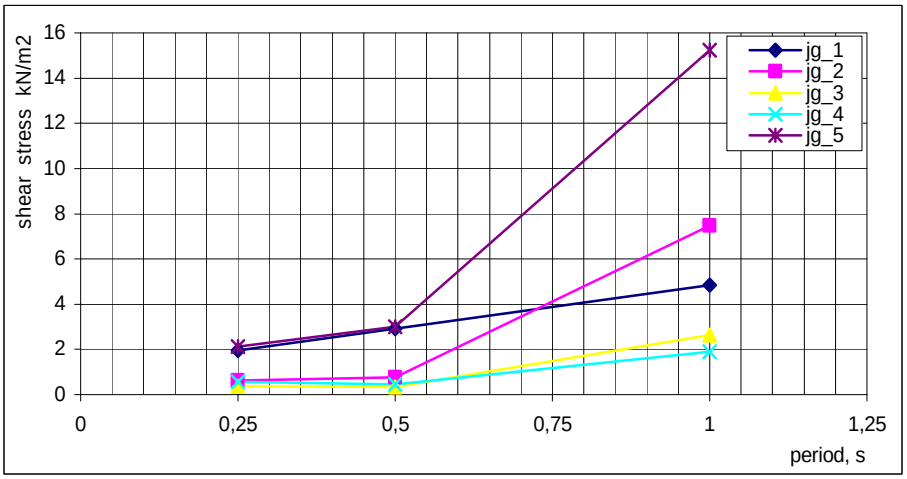

c. capping layer thickness: 30 cm, jg column spacing: 4b

Figure 4.2 Shear stress applied on top of jg columns depending on jg column spacing, capping layer thickness: 30 cm

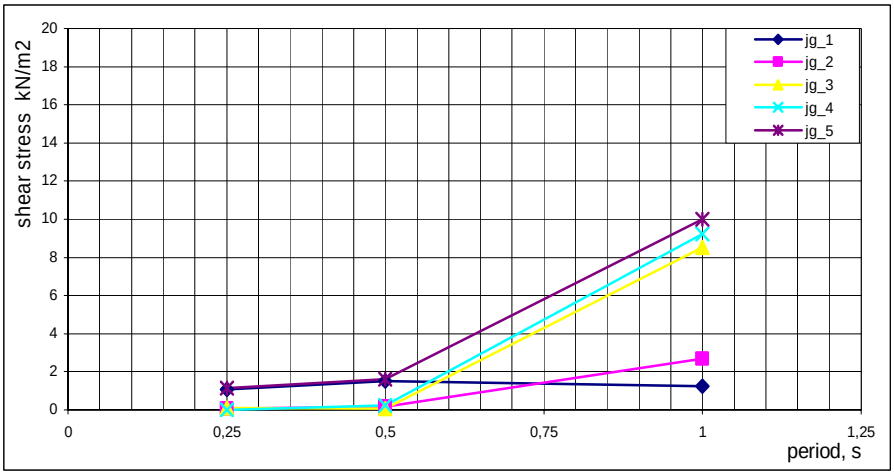

a. capping layer thickness: 50cm, pile interval: 2b

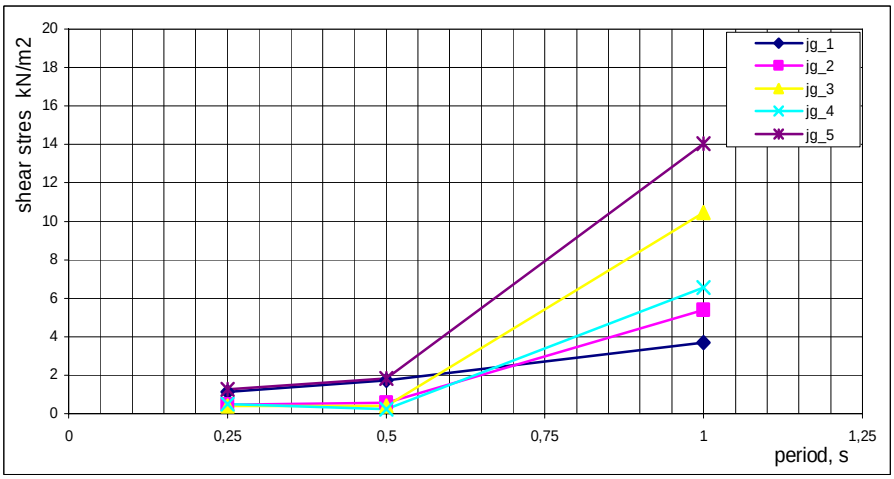

b. capping layer thickness: 50 cm, pile interval: 3b

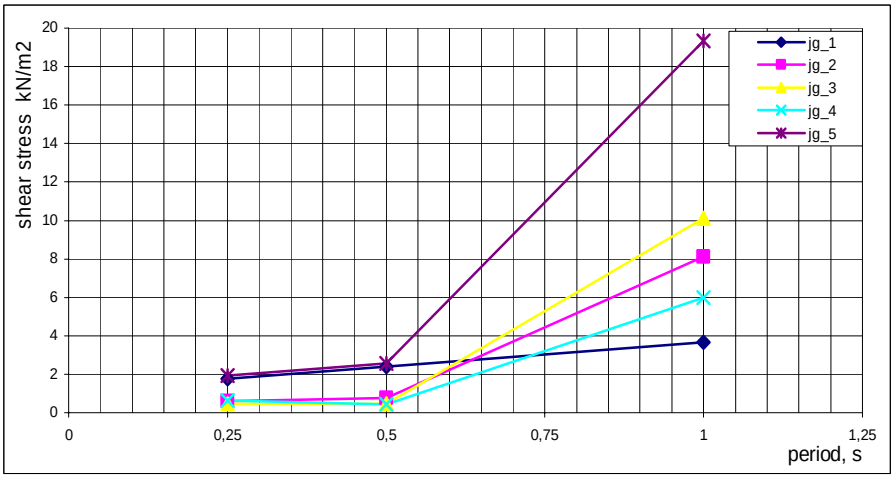

c. capping layer thickness: 50 cm, pile interval: 4b

Figure 4.3 Shear stresses applied on top of jg columns depending on jg column spacing, capping layer thickness: 50 cm

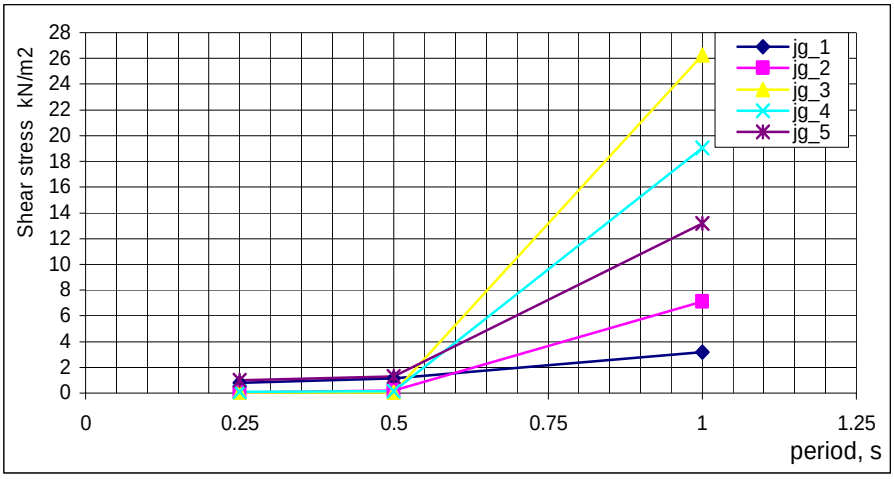

a. capping layer thickness: 70 cm, jg column spacing: 2b

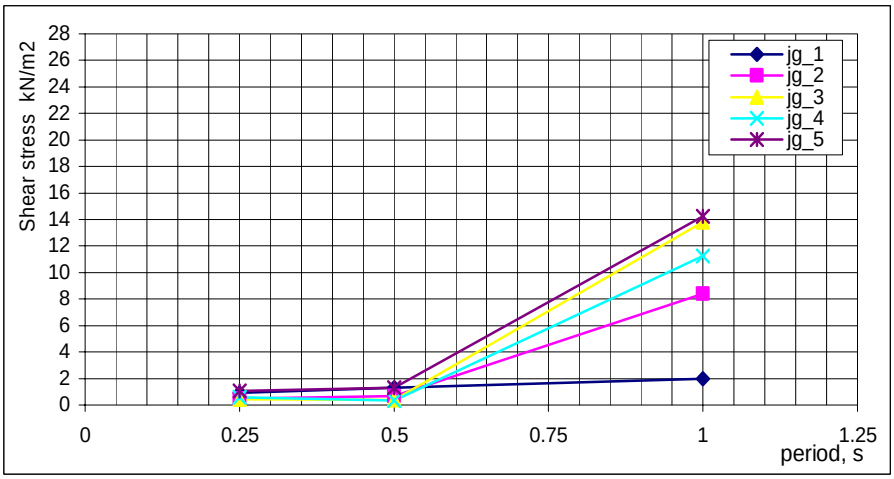

b. capping layer thickness: 70 cm, jg column spacing: 3b

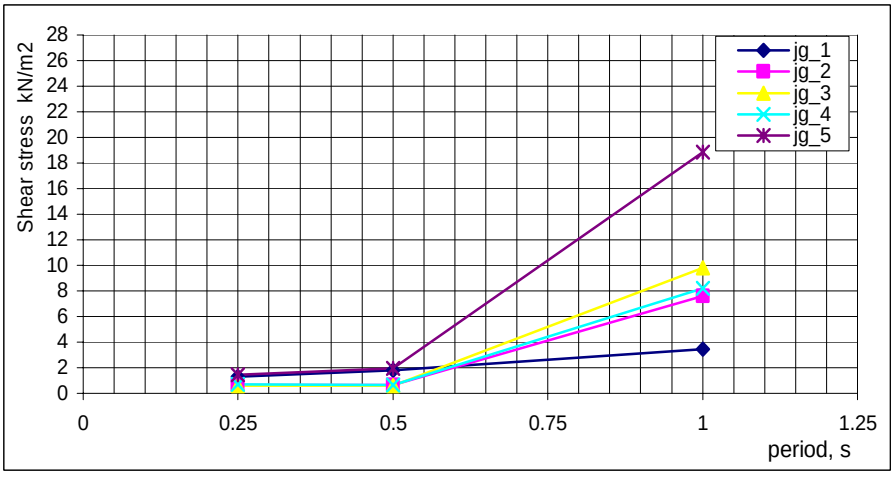

c. capping layer thickness: 70 cm, jg column spacing:4b

Figure 4.4 Shear stresses applied on top of jg columns depending on jg column spacing, capping layer thickness: 70 cm

The period in which the analyses were carried out (T=1.0 s) and the natural period of soil profile model (T=1.1 s) are almost identical, and it has been considered that the ground may be in a resonance condition and behave erratically.

In the second group of figures, capping layer was taken as variable and the periods (T=0.25 s, T=0.50 s, T=1.0 s) are constant. Figures 4.5, 4.6 and 4.7 display the relation between shear stress on top of columns and column spacing.

Increasing the distance between the columns, an apparent increase has been observed in shear stresses on top of columns. These increases can be interpreted by the increase in the effective area per column.

It is seen in these figures that, outer columns take more loads compared with inner columns. However, almost no difference has been observed in the loads on top of inner columns. Therefore, this result should be taken into consideration during project phase of ground improvement operations using jet grout columns.

However, expected results have not been obtained in Figure 4.7 in which period has been taken as T=1.0 s unlike Figure 4.5 and 4.6 in which periods have been taken as T=0.25 s and T=0.50 s. This result could be due to a resonance condition which might have been caused as a result of natural period of soil profile model and Plaxis dynamic analysis period being too close to each other.

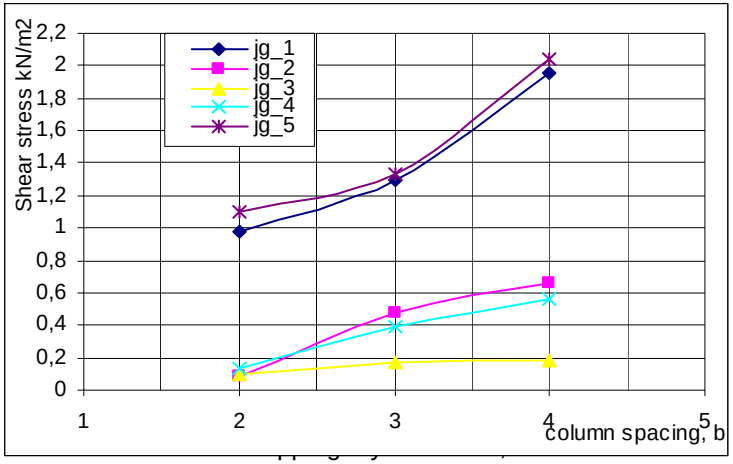

a. Capping layer thickness: 10 cm, T: 0.25 s

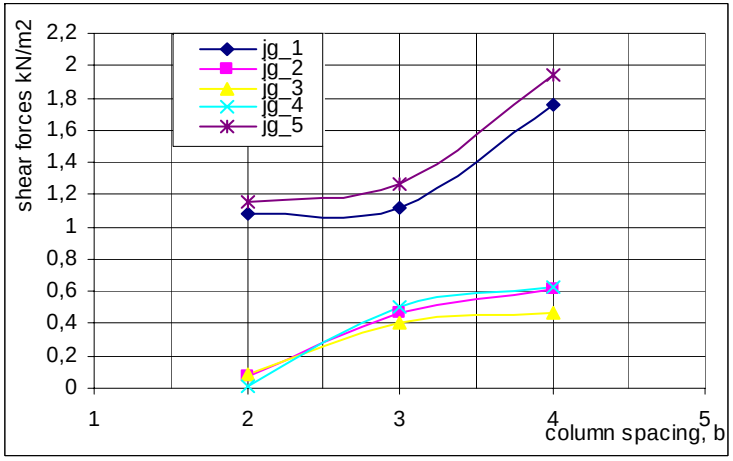

c. Capping layer thickness: 50 cm, T: 0.25 s

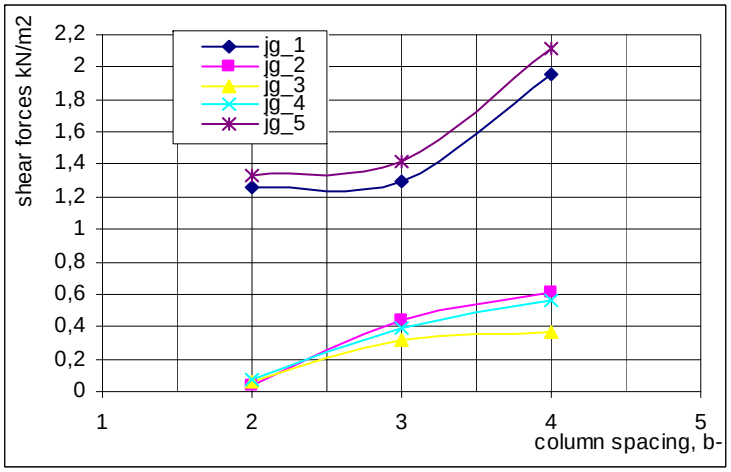

b. Capping layer thickness: 30 cm, T: 0.25 s

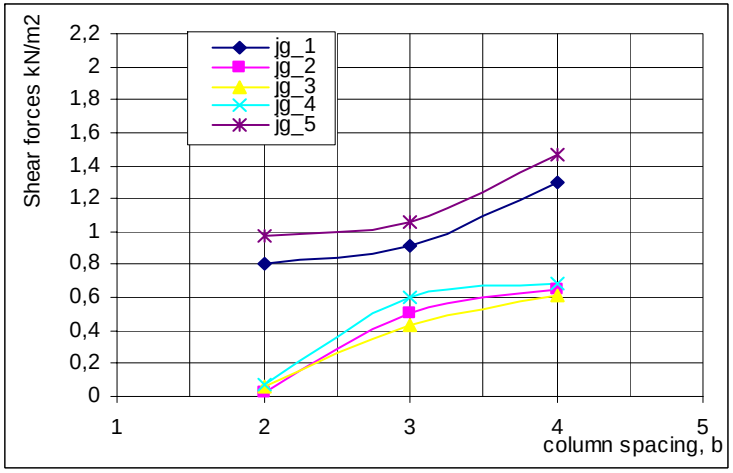

d. Capping layer thickness: 70 cm, T: 0.25 s

Figure 4.5 Shear stresses on top of jg columns in connection with capping layer thickness (period constant T: 0.25 s)

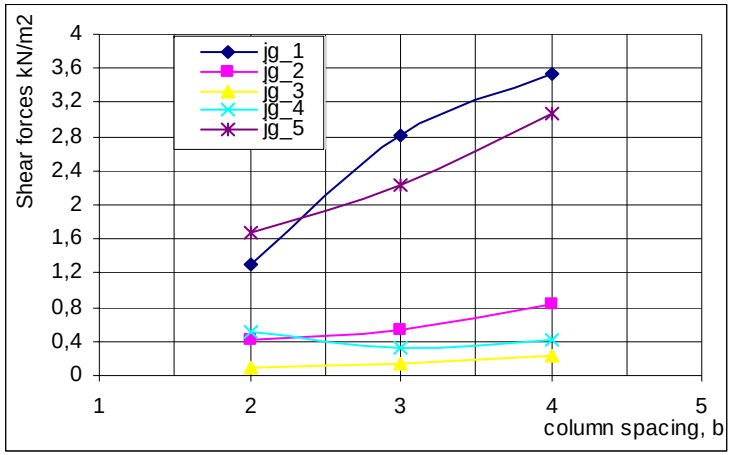

a. Capping layer thickness: 10 cm, T: 0.50s

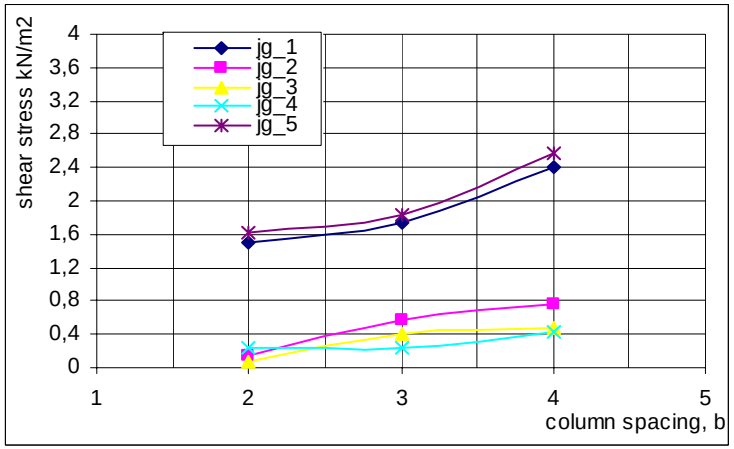

c. Capping layer thickness: 50 cm, T: 0.50 s

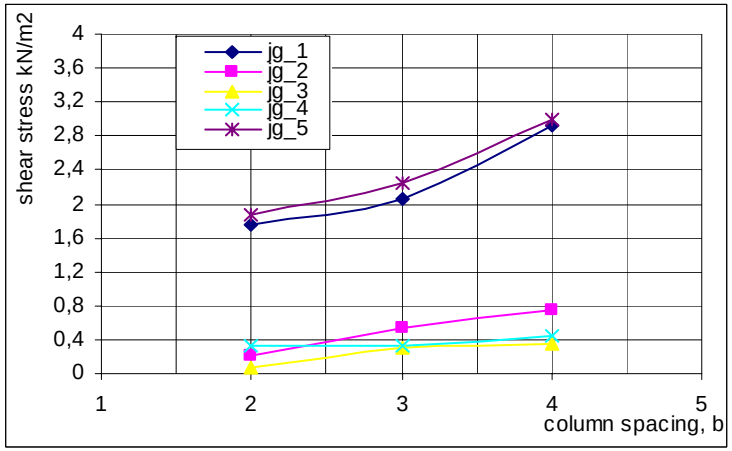

b. Capping layer thickness: 30 cm, T: 0.50 s

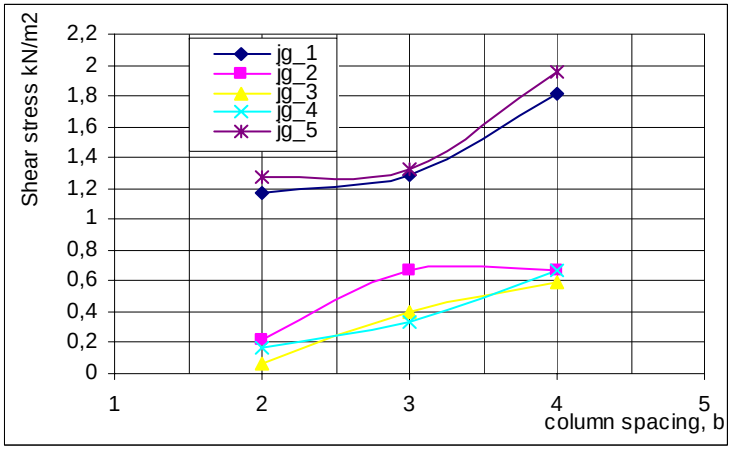

d. Capping layer thickness: 70 cm, T: 0.50 s

Figure 4.6 Shear stresses on top of jg columns in connection with capping layer thickness (period constant T: 0.50)

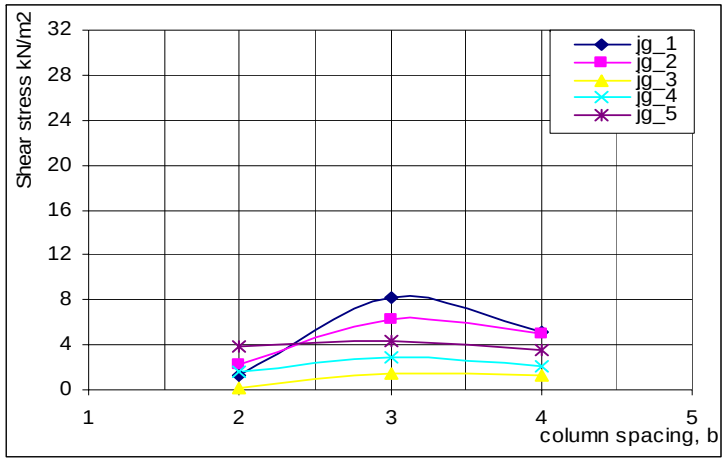

a. Capping layer thickness: 10 cm, T: 1.0 s

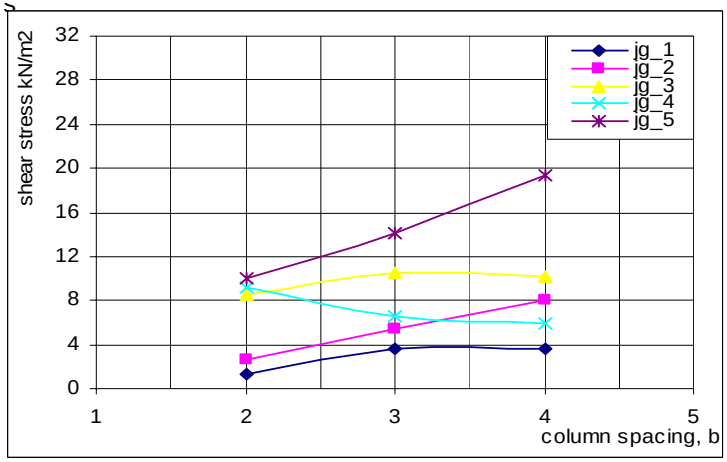

c. Capping layer thickness: 50 cm, T: 1.0s

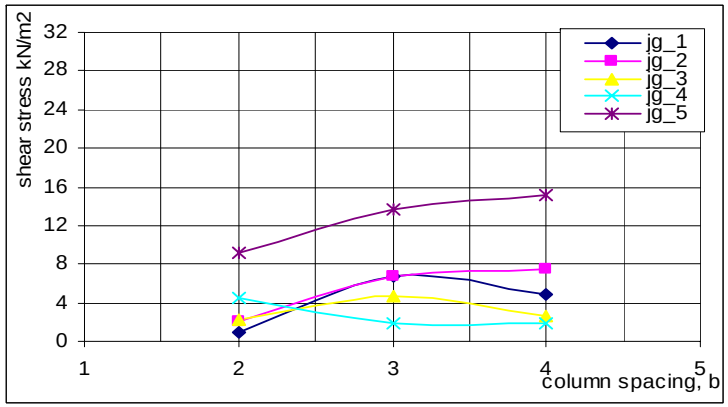

b. Capping layer thickness: 30 cm, T: 1.0 s

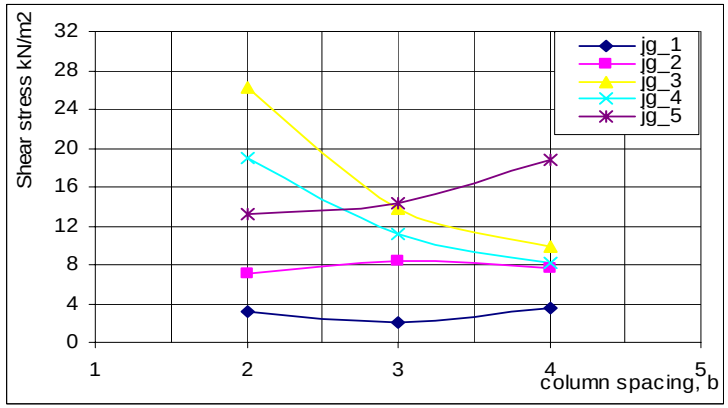

d. Capping layer thickness: 70 cm, T: 1.0 s

Figure 4.7 Shear stresses top of jg columns in connection with capping layer thickness (period constant T: 1.0 s)

In the third group of figures (Figures 4.8, 4.9 and 4.10), the variation of shear stresses were investigated with increase of capping layer thickness while period is constant and column spacing distance is variable.

Depending on the gradual increase of capping layer thickness, a decrease of approximately 35% is recorded with shear stresses applied by the construction on top of jet-grout columns. It means that, capping layer has a damping effect against inertial loads applied on column under lateral dynamic loads. However, the results of analyses in which capping layer were taken as 10 cm are less than the ones in which it was taken as 30 cm. It has been considered that it might be due to a numerical error of the FEM program

.

Another important result is that, group behavior between columns disappears with the increase of column spacing distance, and shear stresses on top of columns increase as shown in Figure 4.8 and Figure 4.9.

In these figures, lateral outer columns receive more shear stress in comparison to inner columns and almost no difference has been determined with shear stress measurements of inner columns.

It can be seen that although Figure 4.8 in which period is T=0.25 s and Figure 4.9 in which period is T=0.50 s are quite similar in form, and pile behavior observed in Figure 4.10 in which period is T=1.0 s is quite different form the other two figures. This is estimated to be the result of resonance condition as mentioned before.

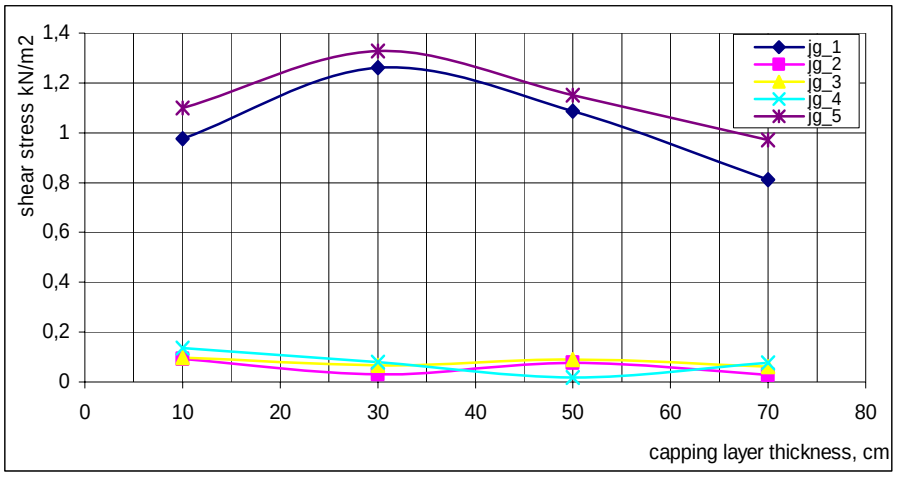

a. jg column spacing: 2b, T: 0.25 s

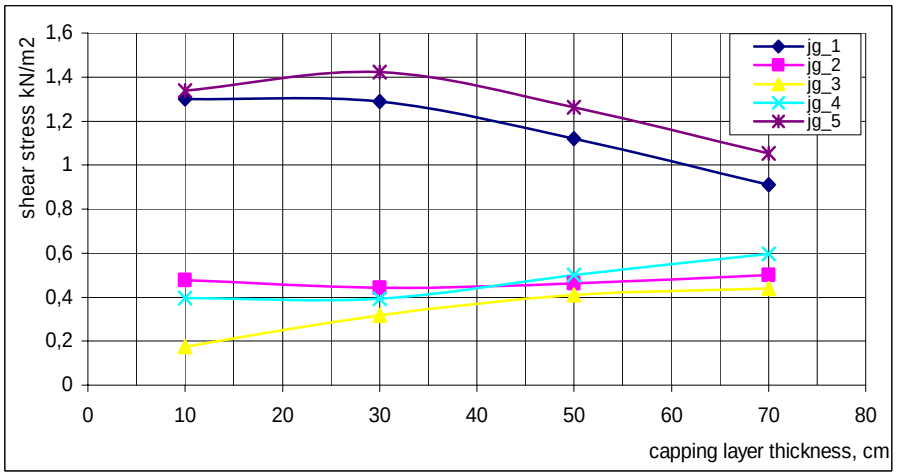

b. jg column spacing: 3b, T: 0.25 s

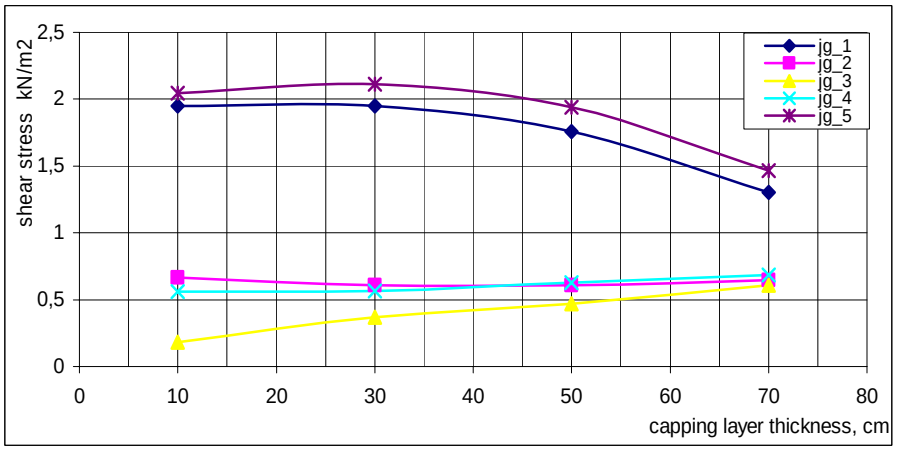

c. jg column spacing: 4b, T: 0.25 s

Figure 4.8 Shear stresses on interface of jg column head depends on jg column spacing, (T: 0.25 s)

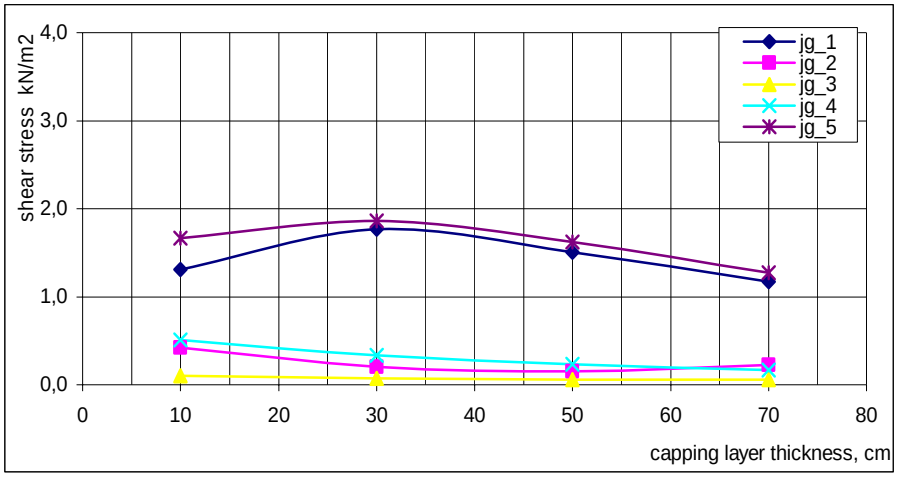

a. jg pile spacing: 2b, T: 0.50 s

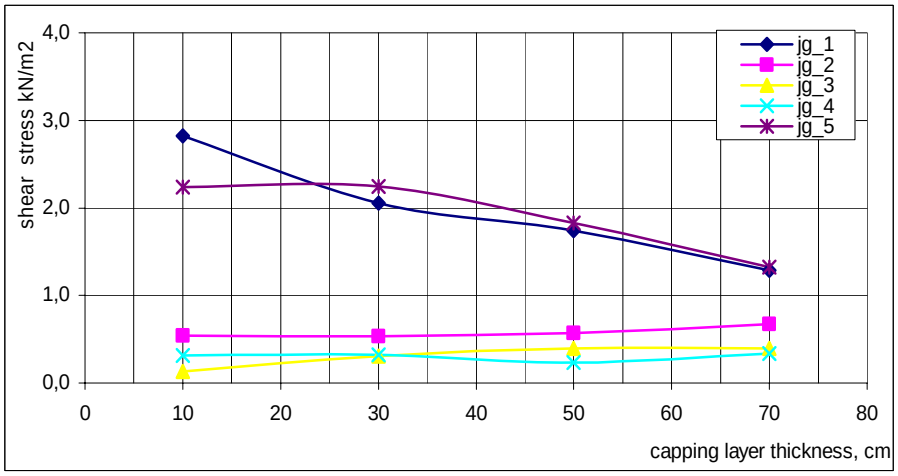

b. jg pile spacing: 3b, T: 0.50 s

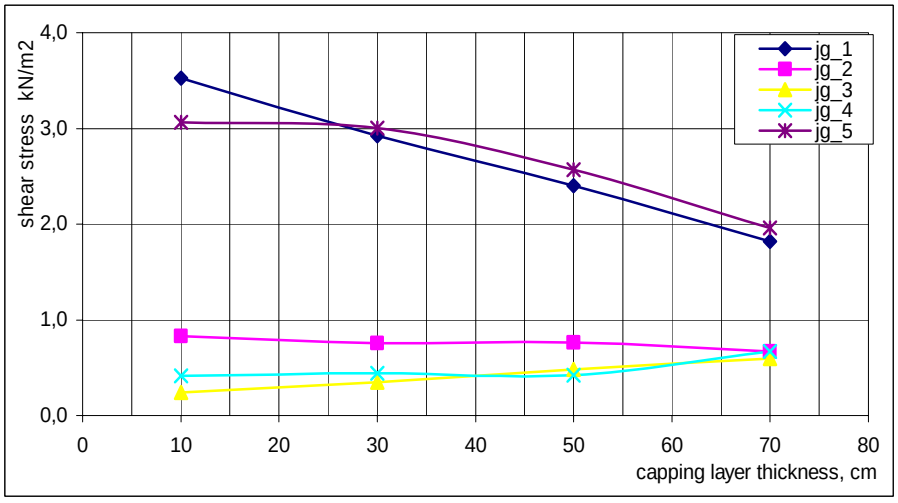

c. jg pile spacing: 4b, T: 0.50 s

Figure 4.9 Shear stresses on interface of jg column head depends on jg column spacing, (T: 0.50 s)

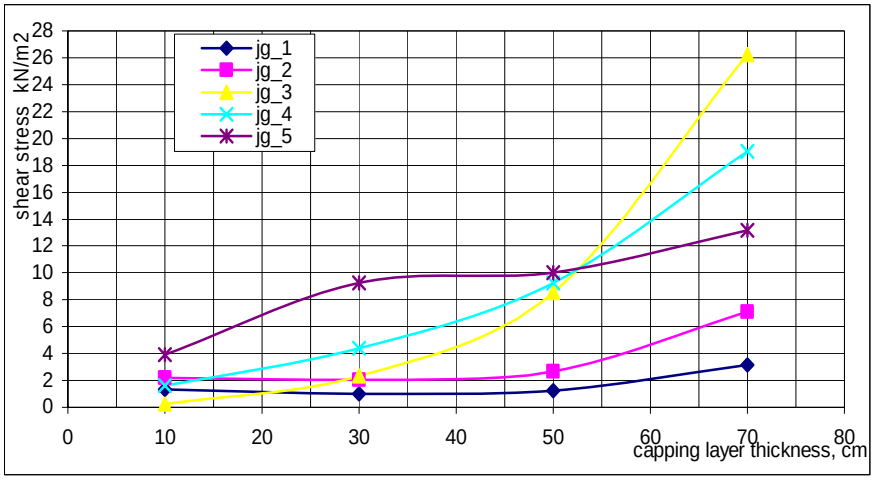

a. Jg column spacing: 2b, T: 1.0 s

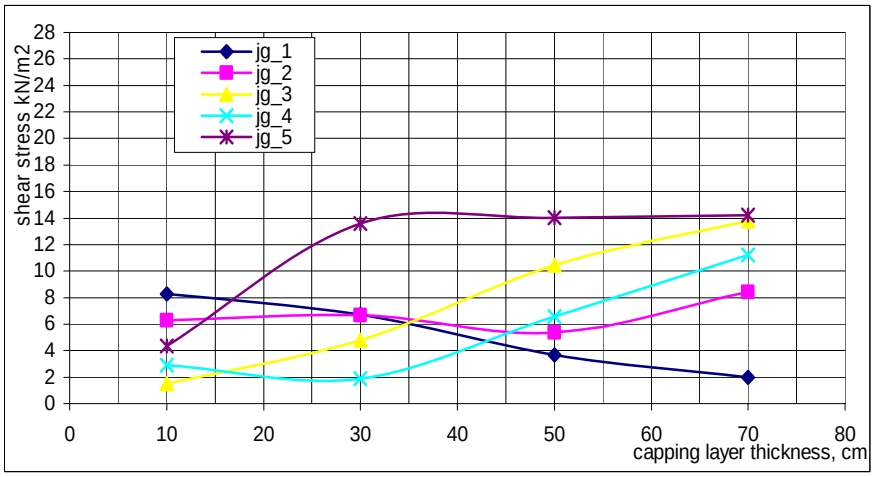

b. Jg column spacing: 3b, T: 1.0 s

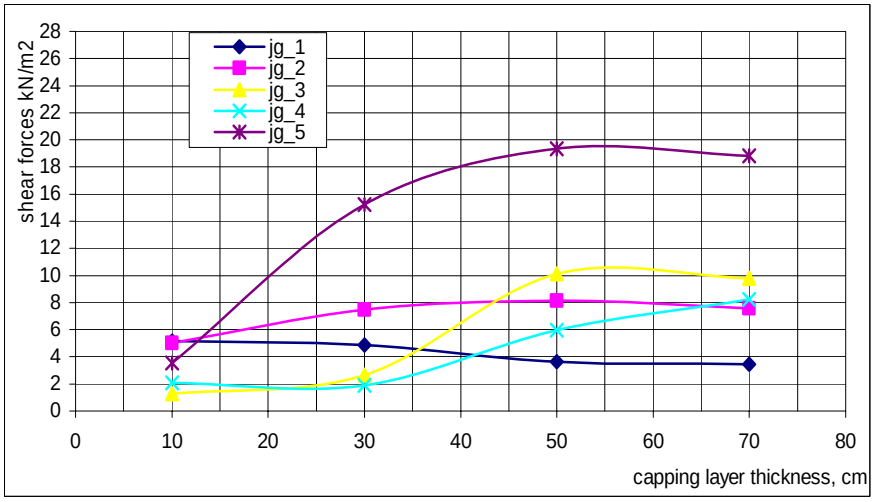

a. Jg column spacing: 4b, T: 1.0 s

Figure 4.10 Shear stresses on interface of jg column head depends on jg column spacing, (T=1.0 sec)

CHAPTER FIVE

CONCLUSIONS

The main goal of this thesis study was to investigate influence of the capping layer on the transfer of inertial lateral loads to jet-grout columns under seismic loading conditions. This investigation is based on a numerical analysis study.

Jet-grouting is a contemporary soil improvement method generally used to increase bearing capacity and foundation resistance of problematic soils. Estimation of axial load carrying capacity of a jet-grout column can be made using pile foundation design principles. However, principles of estimation of lateral load carrying capacity of a jet-grout column have not yet been developed with full confidence. This is because there are some suspicions about lateral load carrying capacity of the jet-grout (JG) columns during earthquakes. This consideration mainly originates from the fact that JG columns do not involve load-carrying reinforcement. On the other hand, there are case histories demonstrating good performance of JG columns during earthquakes. For instance, Soil Crete columns have kept their vertical positions following the Marmara Earthquake although some cracks were observed along the column lengths. This is in contradiction with the results of current analysis procedures. Therefore, the subject needs investigation in order to establish well-defined design procedures and to increase confidence to the jet-grouting method.

A previous study has shown that JG columns may carry kinematical bending moments if they have enough flexural strength. The inertial lateral loads, however, appears to be exceeding lateral load carrying capacity of JG columns according to currently applied analysis methods. It is assumed that bending moments do not take place at the column heads and the shear stress at the bottom of the raft foundation fully acts at the column level in direct proportion to column spacing. This

assumption seems to be over conservative considering the damping potential of the capping layer and positive behavior of the columns in previous earthquakes.

Because of these reasons this thesis study targeted the transfer of inertial loads to the JG columns. The influence of the capping layer was studied in numerical analyses stage of the thesis.

A case history of an industrial plant regarding earthquake performance of JG columns is given in the second chapter of the thesis. It has been demonstrated that JG columns in the Ford Otosan Gölcük Plant did not completely fail during the 1999 Marmara Earthquake. The third chapter is devoted to the statement of the problem and modeling aspects. Results and discussions are given in the fourth chapter. Details of the finite element analyses are presented in the appendix.

Depending on the gradual increase of capping layer thickness, a decrease of approximately 35% is recorded with shear stresses applied by the construction on top of jet-grout columns. It means that, capping layer has a damping effect against inertial loads applied on column under lateral dynamic loads.

Further numerical analyses on this subject may be recommended using spectral accelerations calculated from moderate scale earthquake record instead of harmonic loading conditions. Optimization of the thickness of capping layer can be made studying with different thickness values. JG columns are more flexible than reinforced concrete piles. If the flexibility of JG columns is increased, behavior of these columns may get close to the soil behavior under dynamic loading. This would further increase performance of JG columns under dynamic loading.

REFERENCES

American Petroleum Institute, API. (1980, January). *Recommended Practice for Planning Design and Construction Fixed Offshore Platforms*. API, RP, 2A.

Askay, A. (2002). *Soil Improvement Case Studies Using Jet Grouts. Master of Science Thesis*, Dokuz Eylül Üniversitesi, İzmir, 81 pages

Brinkgreve, R.B.J. (2002) *Plaxis 8.0 User Manual. Plaxis 2D version, 2002)* Delft University of Technology, Plaxis b.v., The Netherlands A.A. Balkema Publishers.

Das, B.M. (1993) *Principal of Soil Dynamics*. Boston, USA. PWS-KENT Publishing Company.

Hayward Baker Company (2005) Retrieved November 20, 2005, from http.//www.haywardbaker.com/services/jet-grouting.htm

Kramer, S.L.(1996) *Geotechnical Earthquake Engineering*. New Jersey, USA Prentice-Hall Civil Engineering and Engineering series.

Nikolau, A.S & G, Gazetas, G. (1997). Seismic design procedure for kinematically loaded piles. Proc. 14th Int. Conf. Soil Mech. Found. Engineering. *Hamburg, Special Volume, ISSMFE TC4 Earthquake geotechnical engineering*, 253-260.

Özsoy, M.B. (2002). *The mitigation of Liquefaction By Means of Soil Improvement Techniques. Doctor of Philosophy Thesis*, İstanbul, 241 pages İstanbul, Türkiye (Boğaziçi University)

Zetaş, Zemin Teknolojisi A.Ş. (2001, July 7) *Vilayetler Birliğine ait İzmir ili Karşıyaka İlçesinde Yaptırılacak Olan Eğitim Tesisleri, Zemin Etüdü ve Değerlendirme Raporu.* İzmir

APPENDIX - A

FINITE ELEMENT MODEL DETAILS

User: Dokuz Eylul University

Title: Jet-grout column analysis

A.1. General Information

Table A.1. Units

Type	**Unit**
Length	m
Force	kN
Time	s

Table A.2. Model dimensions

	min.	max.
X	0.000	150.000
Y	0.000	103.000

Table A.3. Model

Model	Plane strain
Element	15-Noded

A.2. Geometry

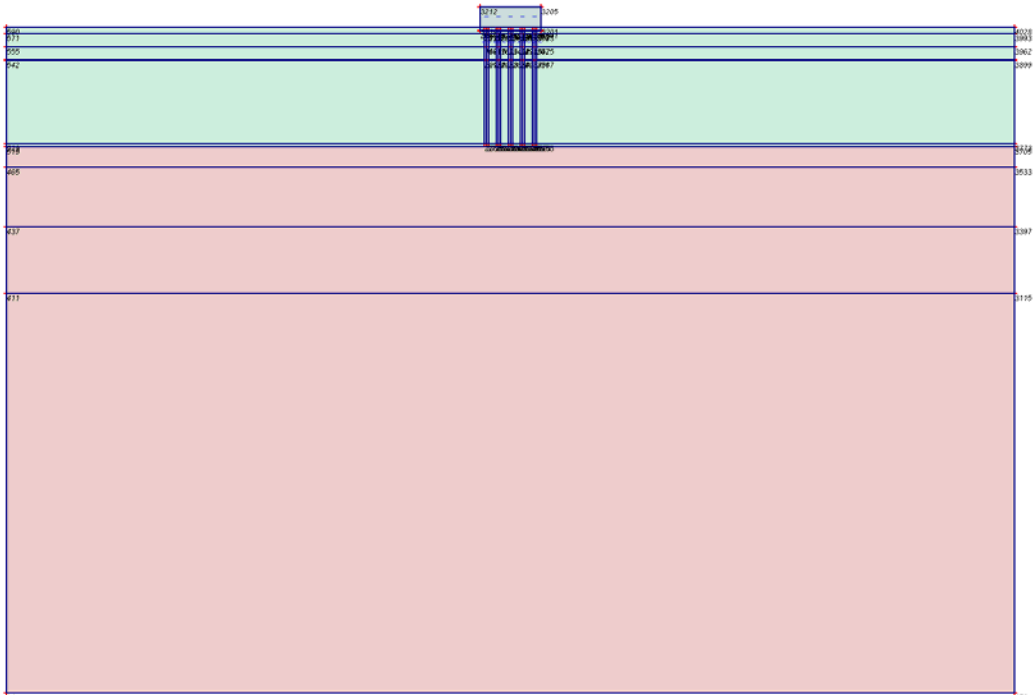

Figure A.1. Plot of geometry model with significant nodes

Table A.4. Table of significant nodes

Node no.	x-coord.	y-coord.	Node no.	x-coord.	y-coord.
590	0.000	100.000	2890	77.100	82.500
4028	150.000	100.000	3185	77.100	99.500
3993	150.000	99.000	2987	77.100	95.000
571	0.000	99.000	3265	78.300	99.500
555	0.000	97.000	3025	78.300	82.500
3962	150.000	97.000	3226	78.300	95.000
542	0.000	95.000	3433	78.900	82.500
3899	150.000	95.000	3481	78.900	99.500
519	0.000	82.000	3517	78.900	95.000
3705	150.000	82.000	2124	71.100	99.000
465	0.000	79.000	2176	71.700	99.000
3533	150.000	79.000	2231	72.900	99.000
437	0.000	70.000	2289	73.500	99.000
3397	150.000	70.000	2364	74.700	99.000
411	0.000	60.000	2929	75.300	99.000
3115	150.000	60.000	2919	76.500	99.000
38	0.000	0.000	2971	77.100	99.000
973	150.000	0.000	3252	78.300	99.000
3219	70.500	100.000	3643	78.900	99.000
2687	70.500	99.500	1715	71.700	97.000
3501	79.500	99.500	1811	73.500	97.000
3201	79.500	100.000	2412	75.300	97.000
2694	71.100	99.500	2945	77.100	97.000
2780	71.100	82.500	3575	78.900	97.000
2099	71.100	95.000	1665	71.100	97.000
2800	71.700	82.500	1761	72.900	97.000
2714	71.700	99.500	2341	74.700	97.000
2156	71.700	95.000	2470	76.500	97.000
2724	72.900	99.500	3242	78.300	97.000
2810	72.900	82.500	2172	71.400	99.500
2192	72.900	95.000	2790	71.400	82.500
2830	73.500	82.500	2279	73.200	99.500
2744	73.500	99.500	2820	73.200	82.500
2263	73.500	95.000	2906	75.000	99.500
2754	74.700	99.500	2850	75.000	82.500
2840	74.700	82.500	2961	76.800	99.500
2305	74.700	95.000	2880	76.800	82.500
2860	75.300	82.500	3491	78.600	99.500
3155	75.300	99.500	3291	78.600	82.500
2396	75.300	95.000	3212	70.500	103.000
3165	76.500	99.500	3205	79.500	103.000
2870	76.500	82.500	529	0.000	82.500
2428	76.500	95.000	3773	150.000	82.500

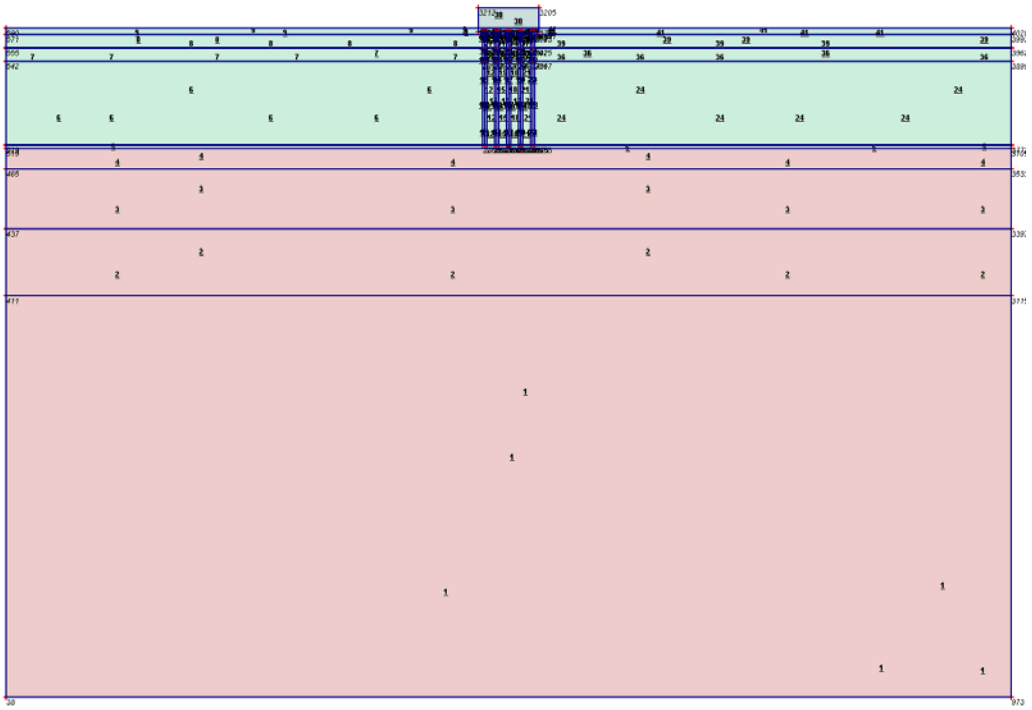

Figure A.2. Plot of geometry model with cluster numbers

Table A.5. Table of clusters

Cluster no.	Nodes
1	411, 3115, 38, 973.
2	437, 3397, 411, 3115.
3	465, 3533, 437, 3397.
4	519, 3705, 465, 3533.
5	519, 3705, 2780, 2800, 2810, 2830, 2840, 2860, 2870, 2890, 3025, 3433, 2790, 2820, 2850, 2880, 3291, 529, 3773.
6	542, 2780, 2099, 529.
7	555, 542, 2099, 1665.
8	571, 555, 2124, 1665.
9	590, 571, 3219, 2687, 2694, 2124.
10	2694, 2780, 2099, 2124, 1665, 2172, 2790.
11	2800, 2714, 2156, 2176, 1715, 2172, 2790.
12	2800, 2156, 2810, 2192.
13	2724, 2810, 2192, 2231, 1761, 2279, 2820.
14	2830, 2744, 2263, 2289, 1811, 2279, 2820.
15	2830, 2263, 2840, 2305.
16	2754, 2840, 2305, 2364, 2341, 2906, 2850.
17	2860, 3155, 2396, 2929, 2412, 2906, 2850.
18	2860, 2396, 2870, 2428.
19	3165, 2870, 2428, 2919, 2470, 2961, 2880.
20	2890, 3185, 2987, 2971, 2945, 2961, 2880.
21	2890, 2987, 3025, 3226.
22	3265, 3025, 3226, 3252, 3242, 3491, 3291.
23	3433, 3481, 3517, 3643, 3575, 3491, 3291.
24	3899, 3433, 3517, 3773.
25	2156, 2192, 1715, 1761.
26	2263, 2305, 1811, 2341.
27	2176, 2231, 1715, 1761.
28	3219, 2687, 3501, 3201, 2694, 2714, 2724, 2744, 2754, 3155, 3165, 3185, 3265, 3481, 2172, 2279, 2906, 2961, 3491.
29	2396, 2428, 2412, 2470.
30	3219, 3201, 3212, 3205.
31	2289, 2364, 1811, 2341.
32	2714, 2724, 2176, 2231.
33	2987, 3226, 2945, 3242.
34	2929, 2919, 2412, 2470.
35	2744, 2754, 2289, 2364.
36	3962, 3899, 3517, 3575.
37	2971, 3252, 2945, 3242.
38	3155, 3165, 2929, 2919.
39	3993, 3962, 3643, 3575.
40	3185, 3265, 2971, 3252.
41	4028, 3993, 3501, 3201, 3481, 3643.

A.3. Structures

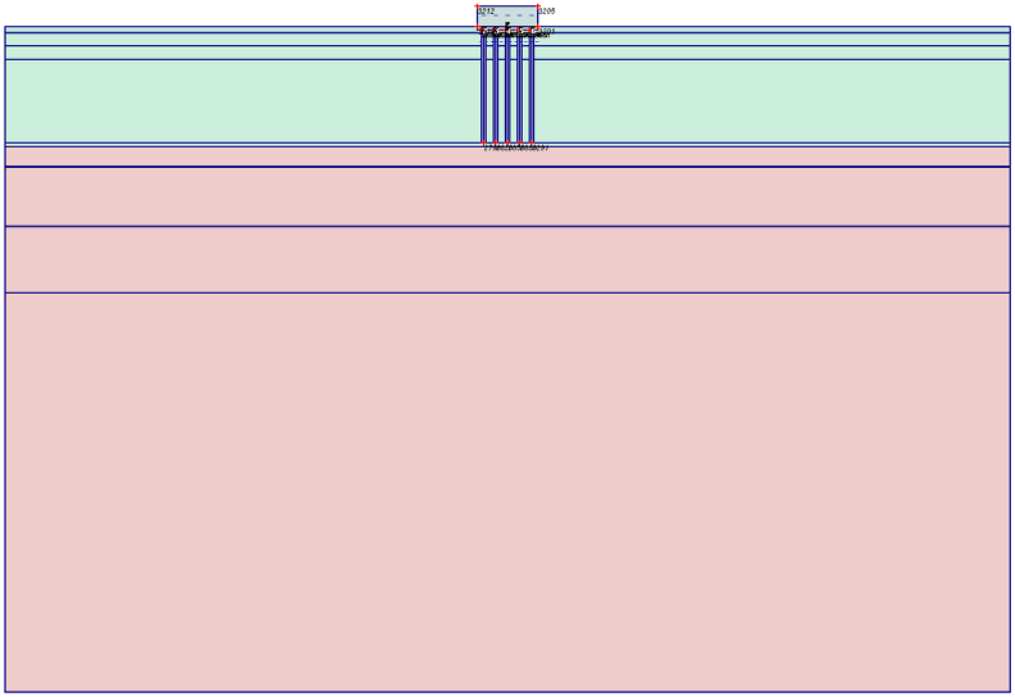

Figure A.3. Plot of geometry model with structures

Table A.6. Beams

Plate no.	Data set	Length [m]	Nodes
1	mat foundation	9.000	3219, 3201.
2	column	3.000	3219, 3212.
3	beam	9.000	3212, 3205.
4	column	3.000	3205, 3201.
5	beam	0.600	2694, 2172, 2714.
6	beam	0.600	2724, 2279, 2744.
7	beam	0.600	2754, 2906, 3155.
8	beam	0.600	3165, 2961, 3185.
9	beam	0.600	3265, 3491, 3481.
10	bar	17.000	2172, 2790.
11	bar	17.000	2279, 2820.
12	bar	17.000	2906, 2850.
13	bar	17.000	2961, 2880.
14	bar	17.000	3491, 3291.

Table A.7. Interfaces

Interface no.	Data set	Nodes
1	zm4	3201, 3219.
2	zm4	2694, 2172, 2172, 2714.
3	zm4	2724, 2279, 2279, 2744.
4	zm4	2754, 2906, 2906, 3155.
5	zm4	3165, 2961, 2961, 3185.
6	zm4	3265, 3491, 3491, 3481.

A.4. Loads & boundary conditions

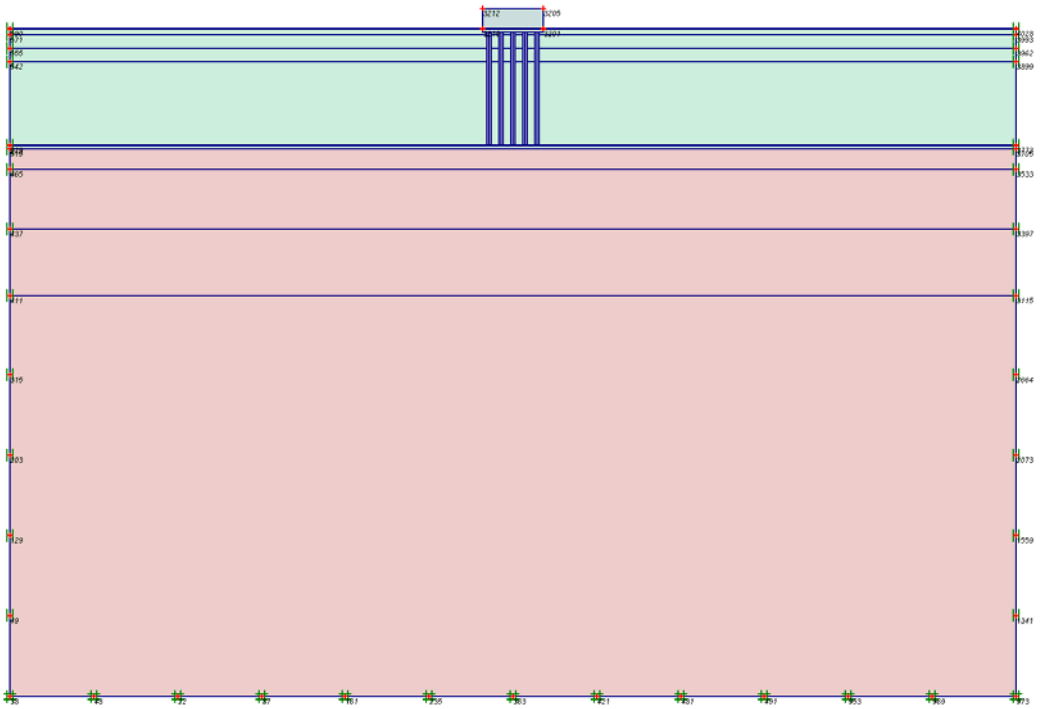

Figure A.4. Plot of geometry with loads & boundary conditions

Table A.8. Node fixities

Node no.	Sign	Horizontal	Vertical	Node no.	Sign	Horizontal	Vertical
38	#	Fixed	Fixed	3899	||	Fixed	Free
973	#	Fixed	Fixed	519	||	Fixed	Free
48	#	Fixed	Fixed	3705	||	Fixed	Free
22	#	Fixed	Fixed	465	||	Fixed	Free
87	#	Fixed	Fixed	3533	||	Fixed	Free
161	#	Fixed	Fixed	437	||	Fixed	Free
235	#	Fixed	Fixed	3397	||	Fixed	Free
363	#	Fixed	Fixed	411	||	Fixed	Free
421	#	Fixed	Fixed	3115	||	Fixed	Free
481	#	Fixed	Fixed	529	||	Fixed	Free
491	#	Fixed	Fixed	3773	||	Fixed	Free
953	#	Fixed	Fixed	315	||	Fixed	Free
969	#	Fixed	Fixed	203	||	Fixed	Free
590	||	Fixed	Free	129	||	Fixed	Free
4028	||	Fixed	Free	49	||	Fixed	Free
3993	||	Fixed	Free	1341	||	Fixed	Free
571	||	Fixed	Free	1559	||	Fixed	Free
555	||	Fixed	Free	2073	||	Fixed	Free
3962	||	Fixed	Free	2664	||	Fixed	Free
542	||	Fixed	Free				

Table A.9. Distributed loads A

Loads no.	First node	qx [kN/m/m]	qy [kN/m/m]	Last node	qx [kN/m/m]	qy [kN/m/m]
1	3219	0.000	0.000	3201	0.000	0.000
2	3212	0.000	0.000	3205	0.000	0.000

Table A.10. Point loads A

Node	Fx [kN/m]	Fy [kN/m]
3219	0.000	0.000
3212	0.000	0.000

A.5. Mesh data

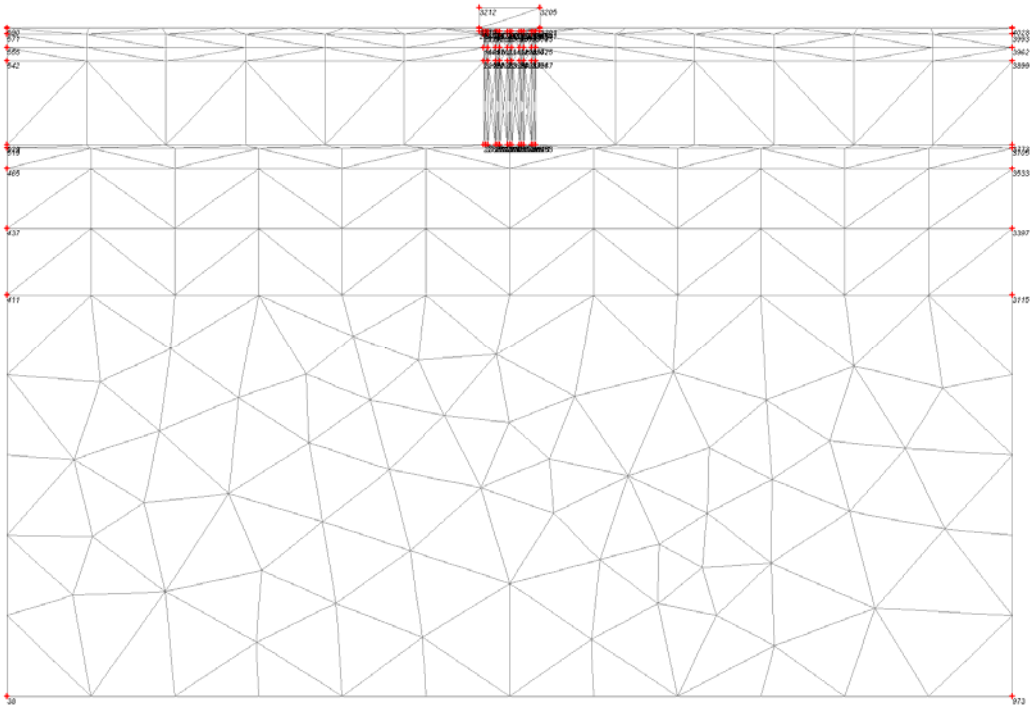

Figure A.5. Plot of the mesh with significant nodes

Table A.11. Numbers, type of elements, integrations

Type	Type of element	Type of integration	Total no.
Soil	15-noded	12-point Gauss	485
Plate	5-node line	4-point Gauss	29
Interface	5-node line	4-point Newton-Cotes	11

A.6. Material data

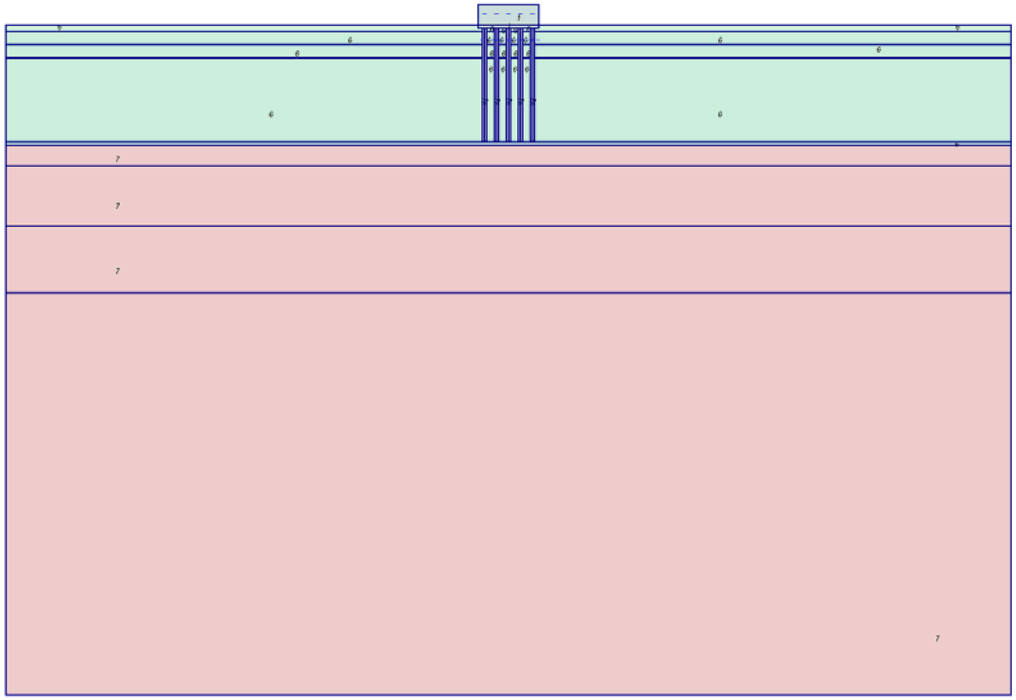

Figure A.6. Plot of geometry with material data sets

Table A.12. Soil data sets parameters

Linear Elastic		**2** **Jg_column**	**6** **zm4**	**7** **zm5**
Type		Non-porous	Drained	Drained
γ_{unsat}	[kN/m³]	23.00	18.08	16.80
γ_{sat}	[kN/m³]	23.00	19.08	17.80
k_x	[m/s]	0.000	1.000	1.000
k_y	[m/s]	0.000	1.000	1.000
e_{init}	[-]	1.000	1.000	1.000
c_k	[-]	1E15	1E15	1E15
E_{ref}	[kN/m²]	1000000.00	158600.00	109500.00
ν	[-]	0.495	0.350	0.350
G_{ref}	[kN/m²]	334448.161	58740.741	40555.556
E_{oed}	[kN/m²]	33779264.214	254543.210	175740.741
E_{incr}	[kN/m²/m]	0.00	0.00	0.00
y_{ref}	[m]	0.000	0.000	0.000
R_{inter}	[-]	0.670	1.000	1.000
Interface permeability		Impermeable	Neutral	Neutral

Mohr-Coulomb		**1 capping_layer**	**3 zm1**	**4 zm2**	**5 zm3**
Type		Drained	Drained	Drained	Drained
γ_{unsat}	[kN/m³]	20.00	18.00	18.00	19.10
γ_{sat}	[kN/m³]	21.00	19.00	19.00	20.10
k_x	[m/s]	1.000	1.000	1.000	1.000
k_y	[m/s]	1.000	1.000	1.000	1.000
e_{init}	[-]	1.000	1.000	1.000	1.000
c_k	[-]	1E15	1E15	1E15	1E15
E_{ref}	[kN/m²]	150000.000	63020.000	63020.000	126400.000
ν	[-]	0.350	0.350	0.350	0.350
G_{ref}	[kN/m²]	55555.556	23340.741	23340.741	46814.815
E_{oed}	[kN/m²]	240740.741	101143.210	101143.210	202864.198
c_{ref}	[kN/m²]	10.00	2.00	2.00	2.00
ϕ	[°]	38.00	30.00	28.00	27.00
ϕ	[°]	0.00	0.00	0.00	0.00
E_{inc}	[kN/m²/m]	0.00	0.00	0.00	0.00
y_{ref}	[m]	0.000	0.000	0.000	0.000
$c_{increment}$	[kN/m²/m]	0.00	0.00	0.00	0.00
$T_{str.}$	[kN/m²]	0.00	0.00	0.00	0.00
$R_{inter.}$	[-]	0.67	1.00	1.00	1.00
Interface permeability		Neutral	Neutral	Neutral	Neutral

Mohr-Coulomb		**8** **zm6**	**9** **zm7**	**10** **zm8**
Type		Drained	Drained	Drained
γ_{unsat}	[kN/m³]	19.37	20.44	20.00
γ_{sat}	[kN/m³]	20.37	21.44	21.00
k_x	[m/s]	1.000	1.000	1.000
k_y	[m/s]	1.000	1.000	1.000
e_{init}	[-]	1.000	1.000	1.000
c_k	[-]	1E15	1E15	1E15
E_{ref}	[kN/m²]	310900.000	514300.000	1054000.000
ν	[-]	0.350	0.350	0.350
G_{ref}	[kN/m²]	115148.148	190481.481	390370.370
E_{oed}	[kN/m²]	498975.309	825419.753	1691604.938
c_{ref}	[kN/m²]	2.00	2.00	2.00
ϕ	[°]	33.00	27.00	28.00
ψ	[°]	0.00	0.00	0.00
E_{inc}	[kN/m²/m]	0.00	0.00	0.00
y_{ref}	[m]	0.000	0.000	0.000
$c_{increment}$	[kN/m²/m]	0.00	0.00	0.00
$T_{str.}$	[kN/m²]	0.00	0.00	0.00
$R_{inter.}$	[-]	1.00	1.00	1.00
Interface permeability		Neutral	Neutral	Neutral

Table A.13. Beam data sets parameters

No.	Identification	EA [kN/m]	EI [kNm²/m]	w [kN/m/m]	□ [-]	Mp [kNm/m]	Np [kN/m]
1	bar	1.314E5	134.57	0.00	0.30	1E15	0.00
2	beam	3.559E7	1.186E7	0.25	0.00	1E15	0.00
3	column	1.067E7	3.203E5	0.00	0.25	1E15	0.00
4	mat foundation	2.373E7	1.35E6	8.50	0.25	1E15	0.00

APPENDIX - B

An Introduction To Plaxis

B.1. Introduction

This chapter briefly introduces usage of Plaxis towards problem of geotechnical. Plaxis is finite element program for geotechnical applications in which soil models are used to simulate the soil behavior. Development of Plaxis began in 1987 at the Technical University of Delft. First of all, Plaxis has been used an easy-to use 2D finite element code for the analysis of river embankments on the soft soils of Lowlands. Incoming years Plaxis was extended to cover most other areas of geotechnical engineering. Today Plaxis can be used for a calculation kernel for 3D calculations.

B.2. Main Goals and Objectives of Usage Plaxis.

Plaxis is intended to provide a tool for practical analysis to be used by geotechnical engineers who are not necessarily numerical specialist. Quite often practicing engineers consider non-linear finite element computations cumbersome and the consuming. Geotechnical applications require advanced constitutive models for the simulation of the non-linear, the independent and anisotropic behavior of silts. In addition since soil is multi-phase material special producers are required to deal with hydrostatic and non-hydrostatic pore pressures in the soil. Although the modeling of soil itself is an important issue many foundation (especially deep foundation and tunnels) projects involve the modeling of structures and the interaction between the structures and the soil. So, nowadays Plaxis is adopted around the world by many geotechnical engineers and it has been using for engineering purposes.

B.3. Graphical Input of Geometry Models.

The input of soil layers, structures, construction stages, loads and boundary conditions is based on convenient CAD drawing procedures, which allows for a detailed modeling of the geometry cross-section. From this geometry model, a 2D finite element mesh is early generated.

B.3.1. General Modeling Aspects

For each new project to be analyzed it is important to create a geometry model first. A geometry model is a 2D representation of a real three dimensional problem and consists of points, lines and clusters. A geometry model should include representative division of the subsoil into distinct soil layers, structural objects, construction stage and loadings. The model must be sufficiently large so that the boundaries do not influence the results of the problem to be studied. The three types of major components in a geometry model are described below.

B.3.1.1. Points.

Points form the start and end of lines. Points can also be used for the positioning of point forces, point fixities and for local refinements of the finite element mesh.

B.3.1.2. Lines.

Lines are used to define the physical boundaries of the geometry, the model boundaries and discontinuities in the geometry such as walls separations of distinct soil layers or construction stages. A line can have several functions or properties.

B.3.1.3. Clusters.

Clusters are areas that fully enclosed by lines. Plaxis automatically recognizes clusters based on the input of geometry lines. Within a cluster the soil properties

are homogenous; hence, clusters can be regarded as part of soil layers. Actions related to clusters apply to all elements in the clusters

After the creation of a geometry model, a finite element model can automatically be generated, based on the composition of clusters and lines in the geometry model.

B.4. Prelimaries on Material Model

The mechanical behavior of soils may be modeled at various degrees of accuracy. Hooke's law of linear, isotropic elasticity, for example; may be thought of as the simplest available stress-strain relationship. As it involves only two parameters, i.e. Young's Modulus, E, and Poisson's ratio,ν it is generally too crude to capture essential features of soil behavior. For modeling massive structural elements and bedrock layer however linear elasticity tends to be appropriate.

B.4.1. Mohr-Coulomb Model

The elastic-plastic Mohr-coulomb model involves five input parameters, i.e., E and ν for soil elasticity; φ and c for soil plasticity and ψ as an angle of dilatency. This Mohr-coulomb model represents a first order approximation of soil behavior. It is recommended to use this model for a first analysis of the problem considered. For each layer on estimates a constant average stiffness. Due to this constant stiffness, computations tend to be relatively fast and one obtains a first impression of deformations. Besides the five model parameters mentioned above, initial soil conditions play an essential role in most deformation problems.

B.5 Input Pre-Processing

To carry out a finite element analysis, a finite element model and specify the material properties and boundary conditions has been to created to constituted model geometry in Plaxis. To set up finite element model, a two dimensional model composed of points, lines and other components, in the x-y plane has to be created by user of Plaxis. The generation of an appropriate finite element mesh and

the generation of properties and boundary conditions on an element level are automatically performed by the Plaxis mesh generator based on input of geometry model. The final part of the input comprises the generation of water pressures and initial stresses to set initial state.

When geometry model is created in the input program it is suggested that the different input items are selected in the order given in Plaxis toolbar. In principle geometry contour was composed then added the soil layers the structural objects, then construction layers, then boundary conditions and than loadings.

B.5.1. The input Program

The input contains all facilities to create and to modify a geometry model, to generate a corresponding finite element mesh and to generate initial conditions. The description is focused on the creation of a geometry model and a finite element mesh

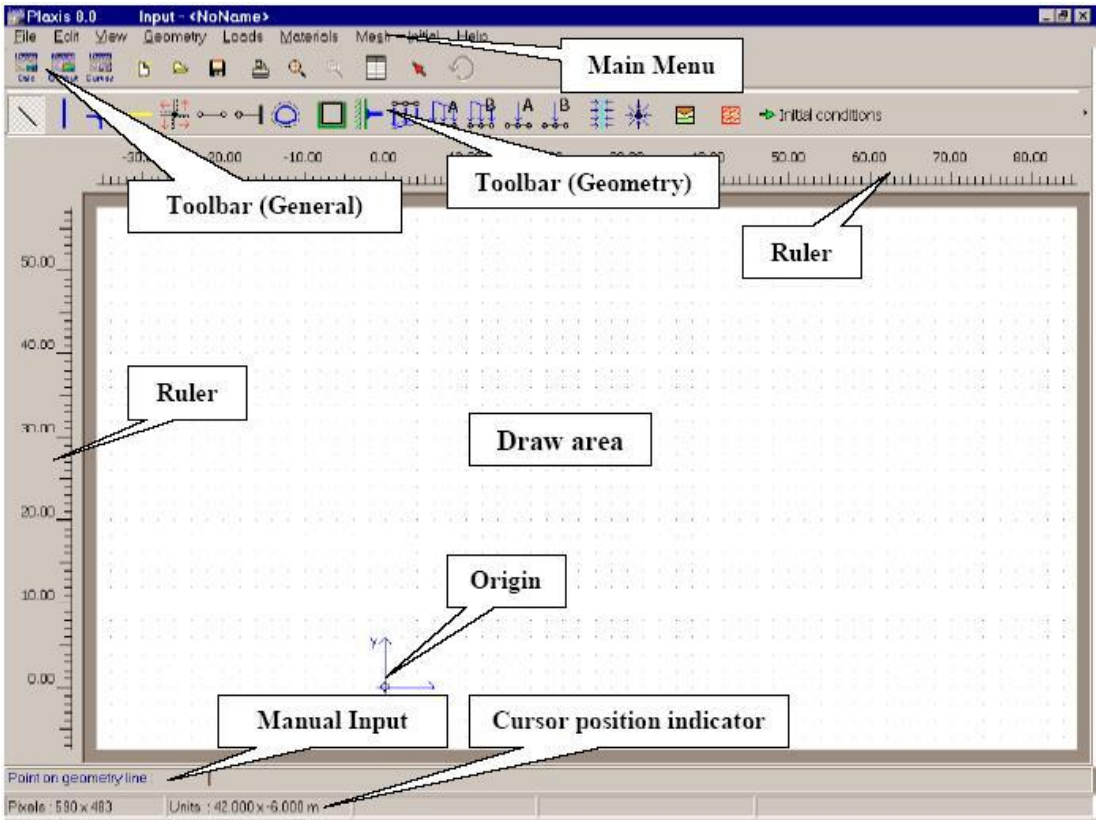

Figure B.1 Plaxis toolbar general view

Finite element models may be either plane strain or axisymmetric plane. A plane strain model is used for geometries with a uniform cross section and corresponding stress state and loading scheme over a certain length perpendicular to the cross section (z-direction). Displacements and strains in z-direction are assumed to be zero. However, Normal stress in z-direction is fully taken into account.

An axisymmetric model is used for circular structures with uniforms radial cross section and loading scheme around the central axis, where deformation and stress state are assumed to be identical in any radial direction note that for axisymmetric problems the x-coordinate represents the radius and the y-coordinate represents to the axial line of symmetry negative coordinates can not be used.

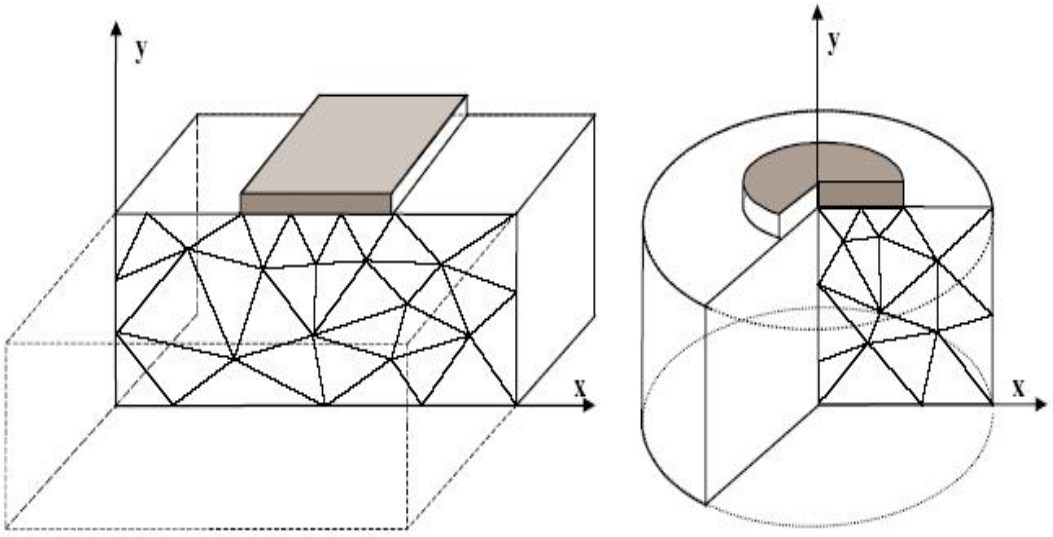

Figure B .2 Example of Plane strain and axisymmetric problem.

B.5.2. Geometry

The geometry of a finite element model begins with the creation of a geometry model which is a representation of the problem of interest. A geometry model consists of points, lines, and clusters. Points and lines are entered by user, whereas clusters are generated by the program. In addition to these basic components, structural objects or special conditions can be assigned to the geometry model to simulate tunnel linings, walls soil structure interaction or loadings.

After the geometry components of the geometry model have been created, the user should compose data sets of material parameters and assign the data sets to the corresponding geometry components. When the full geometry model has been defined and all geometry components have their initial properties the finite element mesh can be generated.

B.5.3. Load and Boundary Conditions

The load sub menu contains the options to introduce distributed loads; line loads are point loads and prescribed displacements in the geometry model. Load and prescribed displacements can be applied at the model boundaries as well as inside the model.

B.5.3.1. Prescribed Displacements.

Prescribed displacements are special conditions that can be imposed on the model control the displacements of certain points. Prescribed displacements can be selected from the loads sub-menu. The input of prescribed displacements in the geometry model is similar to the certain of geometry model is similar to the certain of geometry lines. By default, the input values of prescribed displacements are set such that the vertical displacement components is one unit in the negative vertical direction (u_y=1) and the horizontal displacements component is free.

When prescribed displacements are applied on a line with full fixities the fixities have priority over the prescribed displacements on this line remain zero. Hence, it is not useful to apply prescribed displacements on a line with full fixities.

B.5.3.2. Fixities.

Fixities are prescribed displacements are equal to zero. These conditions can be applied to geometry lines as well as geometry points. In the geometry model, distinction can be made between horizontal fixities (u_Z=0) and vertical fixities

(u_y=0). In addition, one can select total fixities, which is a combination of both (u_y=u_X=0)

B.5.3.3. Standard Fixities

When selecting standard fixities, Plaxis program automatically imposes a set of general boundary conditions are generated according to the following rules. Standard fixities can be used as a convenient and fast option for many practical applications.

Vertical geometry lines for which the x-coordinate is equal to the lowest or highest x-coordinate in the model obtain a horizontal fixity. (u_X=0)

Horizontal geometry lines for which the y-coordinate is equal to the lowest y-coordinate in the model obtain a full fixity (u_y=u_X=0)

Plates that extend to the boundary of the geometry model obtain a fixed rotation in the point at the boundary (ϕ=0). If at least one of the displacement directions of that point is fixed.

B.5.3.4. Distributed Loads

There are two different distributed load systems. (A and B) A and B can be activated indepently. The input values of a distributed load are given in force per area (for example kN/m^2). Distributed loads may consist of an x-and/or y-component. By default, when applying loads to the geometry boundary, the load will be a unit pressure perpendicular to the boundary. The distribution is always linear along line.

On a geometry line where both prescribed displacements and distributed loads are applied, the prescribed displacements have priority over the distributed loads during the calculations, provided that the prescribed displacements are active. Hence, it is not useful to apply distributed loads on a line with fully prescribed displacements.

When only one displacements direction is prescribed whilst the order direction is free. It is possible to apply a distributed load in the free direction.

B.5.3.5. Point Loads

This opinion may be used to create point loads, which are actually line loads in the out-of-plane direction. The input values of point loads are given in force per unit of width. (For example kN/m) Point loads may consist of an x-and/or y-component. By default, when applying point loads, the load will be one unit in the negative y-direction.

The creation of a point or line load in the geometry model is similar to the creation of a geometry point. Two load systems (A and B) are available for a combination of distributed loads and line loads or point loads.

Although the input values of point loads can be specified in the geometry model, the actual value that is applied in a calculation may be changed in the framework of staged construction.

On a part of the geometry where both prescribed displacements and point loads are applied, the prescribed displacements have priority over the point loads during the calculations, provided that the prescribed displacements are active hence, it is not useful to apply points loads on a line with fully prescribed displacements.

B.5.4. Material Properties

Soil prosperities and material properties of structures are stored in material data sets. There are four different types of material sets: data sets for soil & interfaces, plates, geogrids, and anchors. All data sets are stored in a material data base. From the data base, the data sets can be assigned to the soil clusters or to the corresponding structural objects in the geometry model.

B.5.4.1. Data base with material data sets

A material sets window appears showing the contents of the project data base. The project data base contains the material sets for the current project. In addition to the project data base, there is a global data base. The global data base can be used to store material data sets in a global directory and exchange data sets between different projects.

B.5.4.2. Material data sets for soil and interfaces

The material properties and model properties for soil clusters are entered in material data sets. The material properties of interfaces are related to the soil properties and are entered in the same in the soil properties. A data set for soil and interfaces generally represents a certain soil layer and can be assigned to the corresponding clusters in the geometry model. Interfaces that are present in or a long that cluster obtain the same material data set.

Several data sets may be created to distinguish between different soil layers. A user may specify any identification title for a data set. It is advisable to use a meaningful name since the data set will appear in the data base tree view by its identification. For easy recognition in the model, a color is given to certain data set.

The properties in the data sets are divided into three tab sheets: General parameters and interfaces. The general tab sheets contain the type soil model, the type of soil behavior and the general soil properties such as unit weights. The parameters tab sheet contains the stiffness and strength parameters of the selected soil model. The interfaces tab sheet contains the parameters that relate the interface properties to the soil properties.

B.5.5 .Material Model

Plaxis support various models to simulate the behavior of soil and other continua. The model and their parameters are described in detail in the material model manual. Plaxis have same soil models. These are:

- Linear Elastic Model
- Mohr-Coulomb Model
- Jointed Rock Model
- Hardening Soil Model
- Soft soil Model
- Soft Soil Crep Model
- User Defined Soil Model

B.5.6. Type of Material Behavior-Material Type

In principal, all model parameters in Plaxis are meant to represent the effective soil response i.e. The relation between the stresses and strains associated with the soil skeleton an important feature of soil is the presence of pore water. Pore pressures significantly influence the soil response. There are three types of significantly influence the soil response. There are three types of material behavior.

- Drained behavior.
- Undrained behavior
- Non-porous behavior

B.5.7. Type of Material Behavior-Material Type

When the geometry model is fully defined and material properties are assigned to all clusters and structural objects, the geometry has to be divided into finite elements in order to program finite element calculations. A composition of finite elements is called a mesh. The basic type of element in a mesh is the 15-node triangular element or the 6-node triangular element. In addition to these elements, there are special elements for structural behavior. (Plates, geogrids, and anchors). Plaxis allows for a fully automatic mesh generation of finite element meshes. T
he generation of the mesh is based on a robust triangulation procedure which results in unstructured meshes. These meshes may look disorderly, but the numerical performance of such meshes is usually better than for regular (structured) meshes.

The required input for the mesh generator is e geometry model composed of points, lines and clusters, of which the clusters (area enclosed by lines) are automatically generated during the creation of the geometry model. Geometry lines and points may also be sued to influence the position and distribution of elements.